MCDONNELL DOUGLAS TECHNICAL SERVICES CO.
HOUSTON ASTRONAUTICS DIVISION

SPACE SHUTTLE ENGINEERING AND OPERATIONS SUPPORT

DESIGN NOTE NO. 1.4-4-22

DRAG BIAS FEEDBACK FOR THE ANALYTIC DRAG CONTROL ENTRY GUIDANCE SYSTEM

MISSION PLANNING, MISSION ANALYSIS, AND SOFTWARE FORMULATION

---

24 SEPTEMBER 1976

This Design Note is Submitted to NASA Under Task Order No. D0514, Task Assignment A in Fulfillment of Contract NAS9-14960.

PREPARED BY: H. C. Kyle
H. C. Kyle
Engineer
488-5660, Ext. 270

APPROVED BY: J. M. Hiott
J. M. Hiott
Task Manager
488-5660, Ext. 270

APPROVED BY: W. W. Hinton, Jr.
W. W. Hinton, Jr.
Technical Manager -
Flight Analysis
488-5660, Ext. 240

APPROVED BY: W. E. Hayes
W. E. Hayes
Project Manager
Mission Planning, Mission
Analysis & Software Formulation
488-5660, Ext. 266

1.0 SUMMARY

This design note presents a method which corrects the orbiter entry guidance commanded bank angle for biases between navigated drag and guidance computed reference drag. This is accomplished by an integral feedback technique, which uses the drag bias information to adjust the difference between navigated and reference altitude rate used by the Analytic Drag Control (ADC) guidance. The method improves the capability of the ADC guidance system by compensating for any error source which causes a bias between the navigated drag and reference drag profile. These errors include navigated altitude rate errors, atmosphere dispersions, and roll attitude deadband effects. A discussion of the method and results of digital computer entry simulations are presented in this note.

2.0 INTRODUCTION

The Analytic Drag Control (ADC) entry guidance has been developed and baselined for the space shuttle orbiter entry (Reference A). This system controls the entry trajectory by roll modulation while using a pre-selected angle of attack profile that is a function of relative velocity. The vehicle is controlled to maintain a reference drag acceleration-velocity (D-V) profile from entry interface (400,000 feet altitude) to the point of Terminal Area Energy Management (TAEM).

The design D-V profile is shaped pre-mission to optimize the various entry parameters including surface temperatures, backface temperatures, structural loads, vehicle lift/drag (L/D) capabilities, and TAEM interface position and velocity. In designing the D-V profile for a given mission, each of these constraints is defined in the D-V plane. Adequate margins must be allowed from the constraint boundaries to provide for dispersions in aerodynamics, atmosphere, entry interface conditions, winds, navigation system errors, etc. During the entry, the guidance system computes a reference drag value each guidance cycle as well as the bank angle required to fly this reference. Under ideal conditions, this commanded bank angle causes the vehicle to fly the reference D-V profile which in turn closely follows the design profile. If some dispersion causes the navigated drag not to follow the reference drag profile, the reference profile being computed each guidance cycle is adjusted to assure correct range at TAEM interface.

In order to minimize the required design trajectory margins and allow for trajectory optimization, it is essential that the guidance system capability enable the navigated drag to closely follow the reference drag profile. Certain dispersions can cause the navigated drag to incur a bias with respect to the reference which cannot be corrected by the guidance. This proposed method to alleviate this problem uses the concept of integral feedback to apply a correction to the ADC guidance-controller equation.

3.0 DISCUSSION

The ADC guidance outputs the commanded bank angle each guidance cycle according to the following equations:

$$\phi_C = \cos^{-1}\left[\frac{(\frac{L}{D})_V}{(\frac{L}{D})}\right] \times RK2ROL$$

where

ϕ_C = commanded vehicle bank angle

$(\frac{L}{D})$ = total navigated vehicle lift/drag

$(\frac{L}{D})_V$ = commanded vertical component of vehicle L/D

RK2ROL = ± 1 (determines roll direction for crossrange correction)

$(\frac{L}{D})_V$ is computed as follows:

$$(\frac{L}{D})_V = (\frac{L}{D})_r + C16\ (D-D_r) + C17\ (\dot{R}_r - \dot{R})$$

where

$(\frac{L}{D})_r$ = reference lift/drag computed by the guidance

D = navigated drag acceleration

D_r = reference drag acceleration

$\dot{R}_r$ = reference altitude rate

$\dot{R}$ = navigated altitude rate.

C16, C17 are defined functions of drag acceleration (Reference A).

A major error source in the $(\frac{L}{D})_V$ equation is in the value used for navigated altitude rate. Errors on the order of 50 - 100 feet/second in $\dot{R}$ cause significant deviations of the commanded bank angle from that required to maintain the reference drag profile.

The integral feedback correction method under study assumes that a primary objective is to insure that the navigated drag follows the reference. In order to accomplish this, a term $K(D-D_r)$ may be used as a feedback correction to the $(\frac{L}{D})_V$ equation. Since these errors are generally slowly changing, once the proper bias correction is determined and applied to the $(\frac{L}{D})_V$ calculation, the drag will properly follow the reference. Since the correction is considered to affect the $(\dot{R}_r-\dot{R})$ term, this bias correction can be written as

$$\Delta\dot{R} = \Delta\dot{R}_{PREVIOUS} + K\,(D-D_r)$$

and is updated each guidance cycle. The controller equation is amended to read

$$(\frac{L}{D})_V = (\frac{L}{D})_r + C16\,(D-D_r) + C17\,(\dot{R}_r - (\dot{R} + \Delta\dot{R}))$$

The effect of this $\Delta\dot{R}$ correction is to integrate the area between the drag and reference drag curves and to convert this dynamic value to an equivalent altitude rate error. If the navigated drag curve crosses over the reference drag curve, the sign of the new $\Delta\dot{R}$ increment is reversed. Thus the total $\Delta\dot{R}$ tends to stabilize at the value which causes the bias. It should be noted that while the correction is applied to the $\dot{R}$ value, the feedback method will correct for any error source which causes a bias in the drag-velocity profile.

Error Sources Considered

In checkout of this method, an error in $\dot{R}$ was investigated in Space Vehicle Dynamics Simulation (SVDS) entry simulations (Reference B).

This was accomplished by setting a platform pitch misalignment error such that $\dot{R}$ was up to $\pm$240 feet/second in error (from $\dot{R}$ actual). Combined dispersion cases were also run including platform pitch misalignment, headwind/tailwind, and aerodynamics dispersions. Atmospheric dispersion effects were simulated by using January and July atmosphere models.

Gain Selection

Using these error sources, a range of values for the gain, K, was considered to determine the best gain for the correction term. Two basic methods were considered for use as to the integration technique. Of primary consideration in the overall design was method simplicity and efficient use of onboard software core allocation.

One method, designated method A in the attached figures, utilizes a large (constant) value for K, performing the summing operation only when the navigated drag is diverging from the reference drag. Whenever the drag is converging to the reference, K is set to zero. Roll reversals result in differences between the reference and navigated drag acceleration that are of a transient nature rather than a bias. Because of this, the integrator is turned off at the start of a roll reversal for a period of 80 seconds. Since the errors being considered are generally of a slowly changing nature, turning the integrator off for this time period causes very little error in the $\Delta\dot{R}$ correction term. This allows sufficient time for the drag to begin re-converging to the reference profile for any roll reversal. The convergence then causes the integrator to

remain off until the drag again diverges from the reference.

Another situation which must be considered is that period during which the roll command is being constrained by some preset limit. In such a case, the drag may diverge from the reference profile due to the roll limit rather than due to errors compensated for by the integral feedback method. This situation is covered by holding $\Delta\dot{R}$ constant during the time that the roll command is limited in this manner.

Values of K ranging from 1.0 - 6.0 were tested with various error sources using this method. Good response, based on effective correction to the reference without overcontrolling was seen with values of K between 2.0 and 4.0. These values induce sufficient lag in the $\Delta\dot{R}$ correction and avoid overreaction to trajectory transients.

A second method, method B, involves using a relatively small value for K, keeping the integrator on whether the drag is diverging or converging to the reference profile. In this method, the integrator is again turned off for a specified time after a roll reversal begins. Since the total time required for the roll-reversal-caused drag divergence/convergence varies depending on drag level, velocity, and initial bank angle, the integrator is turned off for a nominal time period (80 seconds). The exact time off is not critical since the error is slowly changing and since the gain is relatively small. The roll-limited situation is handled in the same manner

as in method A. Best results were obtained with K = 1.0 using this method.

An example case illustrating the integral feedback method is presented in Figures 1 and 2. Figure 1.1 shows the drag-velocity profile for Trajectory Number 60412 (OFT-1) with a seasonal (January) atmosphere model incorporated into the SVDS simulation. This atmosphere model results in the drag-reference drag bias shown. Using the method A $\dot{\Delta R}$ correction produces the results shown in Figure 2.1. The actual $\dot{\Delta R}$ correction applied for this case is shown in Figure 2.2. The major deviations from the reference drag profile are the roll reversals which occur at approximately 17500 ft/sec and at 6000 ft/sec. At the start of a roll reversal, the integrator is turned off ($\dot{\Delta R}$ correction remains constant) until the drag reconverges to the reference.

A second example is presented in Figures 3 and 4. Figure 3.1 shows the bias caused by the vehicle roll attitude deadband. This case sets the actual roll angle a constant 5° greater than the roll command. This represents the extreme case in which the actual roll angle maintains the limit of a 5° roll angle deadband throughout the trajectory. Figure 4.1 shows the drag profile using the $\dot{\Delta R}$ correction method A. The actual $\dot{\Delta R}$ correction applied is shown in Figure 4.2.

A problem area is apparent during the transition entry phase from a relative velocity of approximately 8000 feet/second to TAEM

interface. During this time, the navigation system is subject to large updates due to TACAN acquisition and barometric altimeter inputs. These normally serve to reduce the navigation errors in altitude rate faster than the drag feedback method can adjust. This suggests the need for a variable gain or some additional technique for correction during this period. In the cases shown, $\Delta\dot{R}$ was ramped to reach zero at 180 seconds after TACAN acquisition. If TACAN is interrupted after initial acquisition, integration of $(D\text{-}D_r)$ is resumed. This allows $\Delta\dot{R}$ to approximate ($\dot{R}$ actual - $\dot{R}$ nav) for the cases studied. Additional study is required in this area.

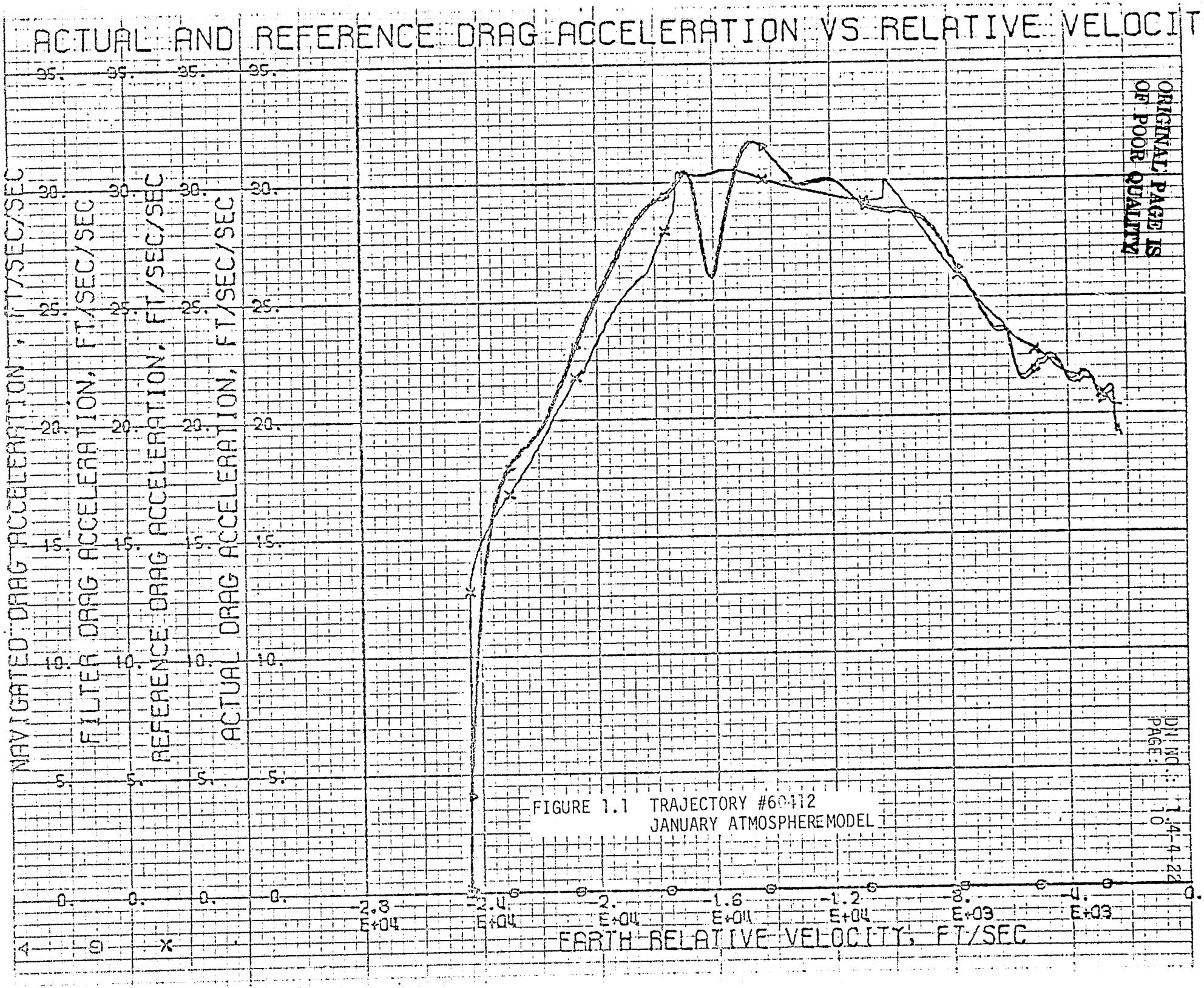

FIGURE 1.1 TRAJECTORY #60412
JANUARY ATMOSPHERE MODEL

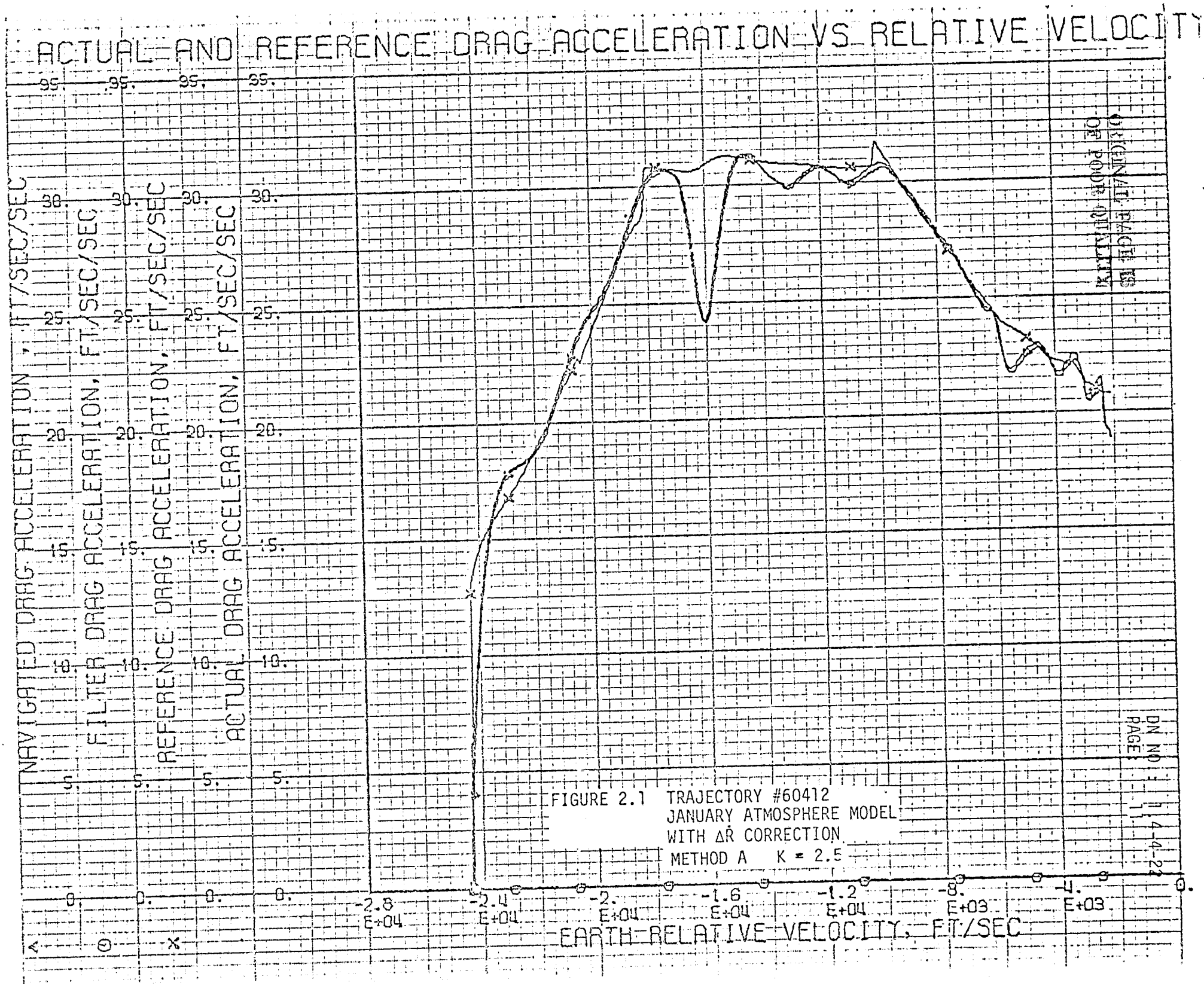

FIGURE 2.1 TRAJECTORY #60412
JANUARY ATMOSPHERE MODEL
WITH $\Delta\dot{R}$ CORRECTION
METHOD A K = 2.5

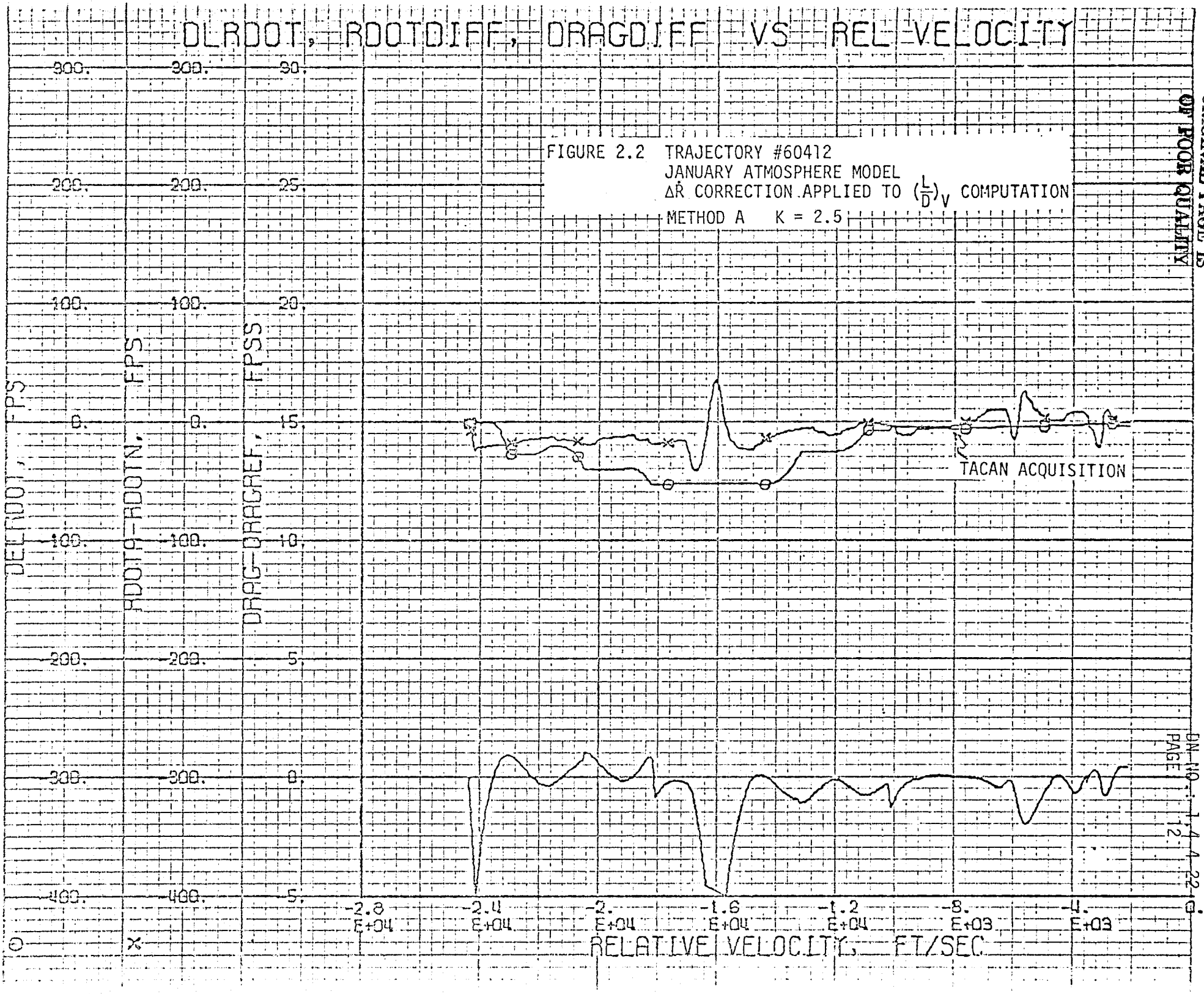

ORIGINAL PAGE IS
OF POOR QUALITY

BN NO. 1-4-4-22-6
PAGE 12

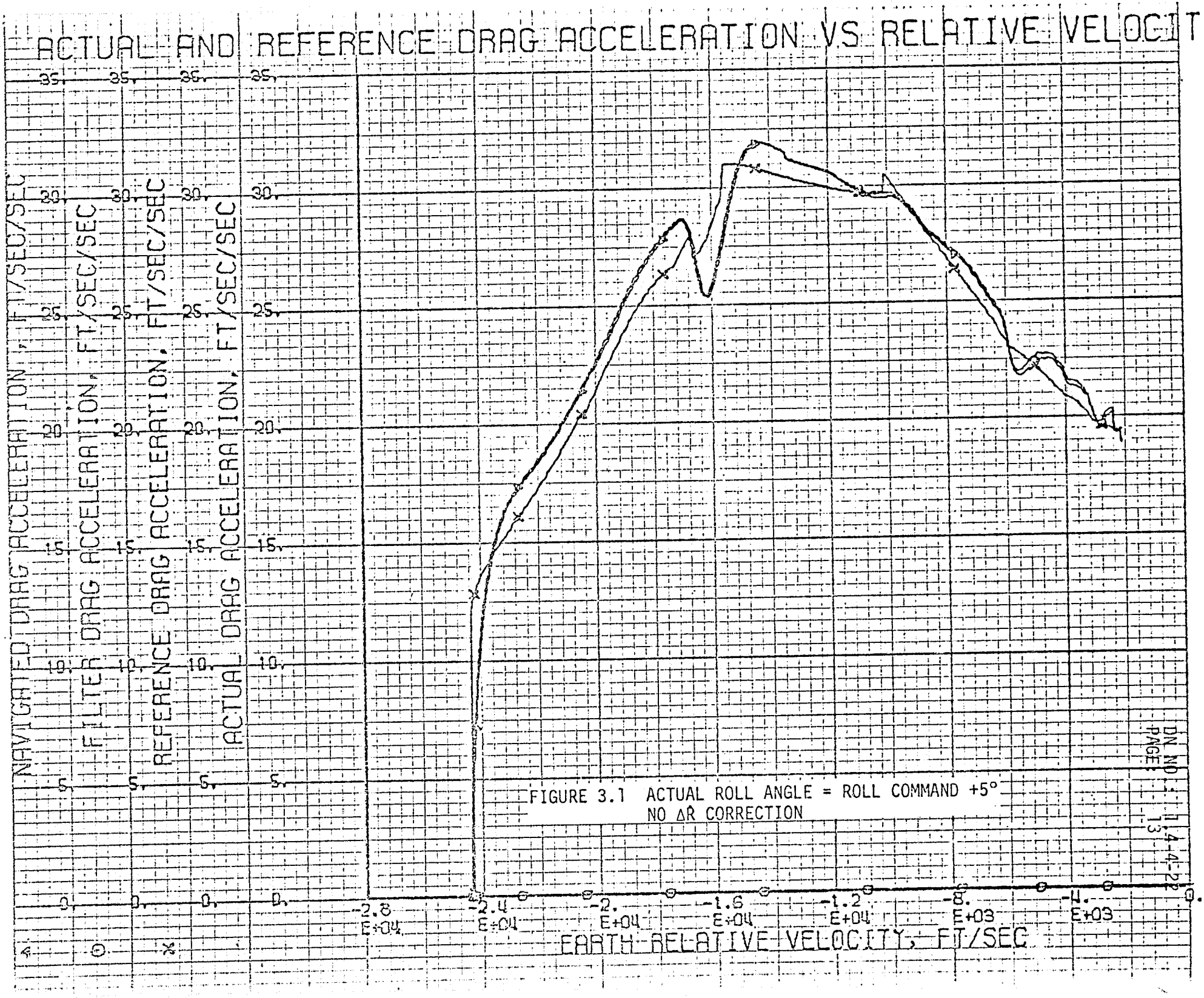

FIGURE 3.1 ACTUAL ROLL ANGLE = ROLL COMMAND +5°
NO ΔR CORRECTION

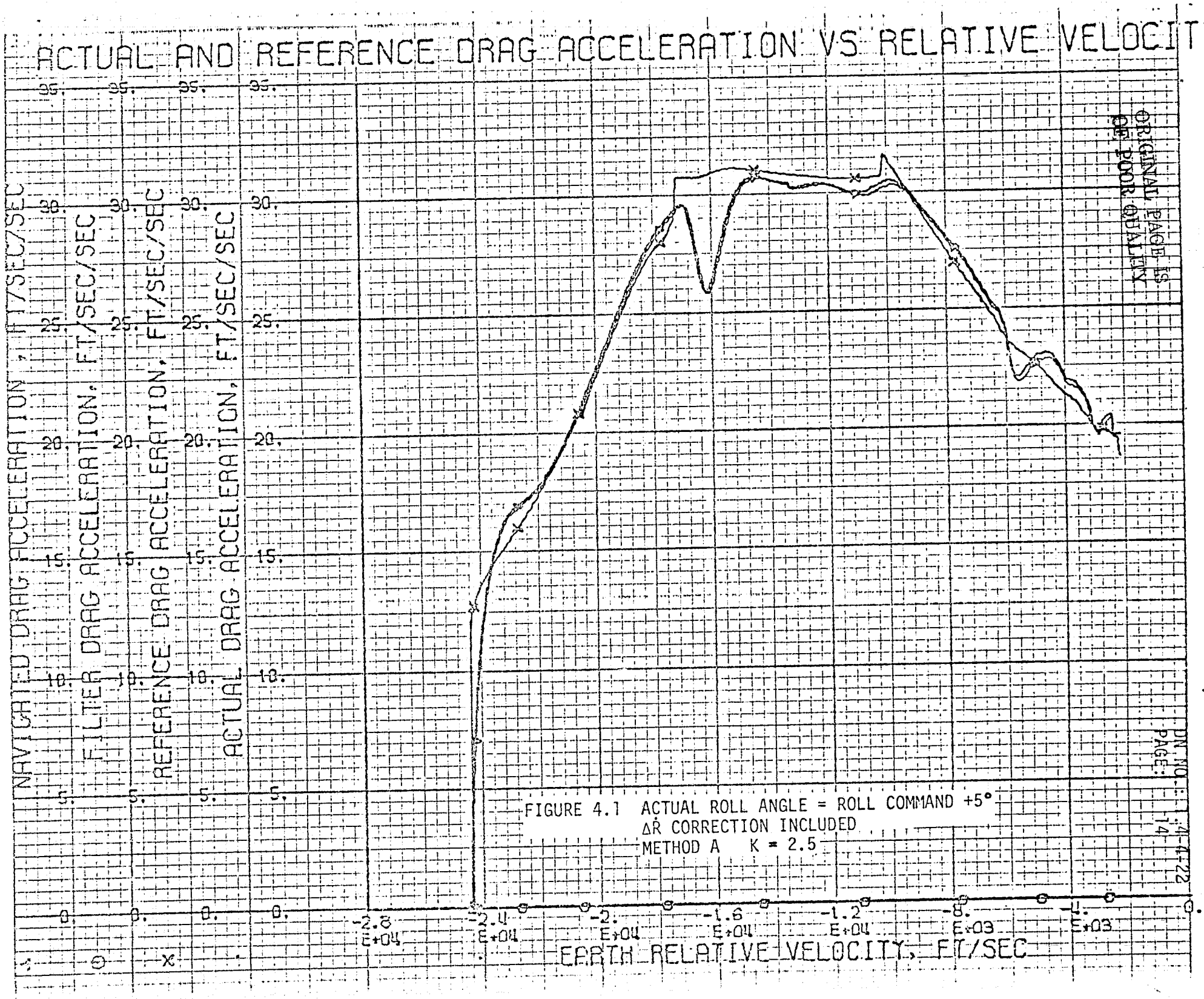

FIGURE 4.1 ACTUAL ROLL ANGLE = ROLL COMMAND +5°
$\Delta\dot{R}$ CORRECTION INCLUDED
METHOD A K = 2.5

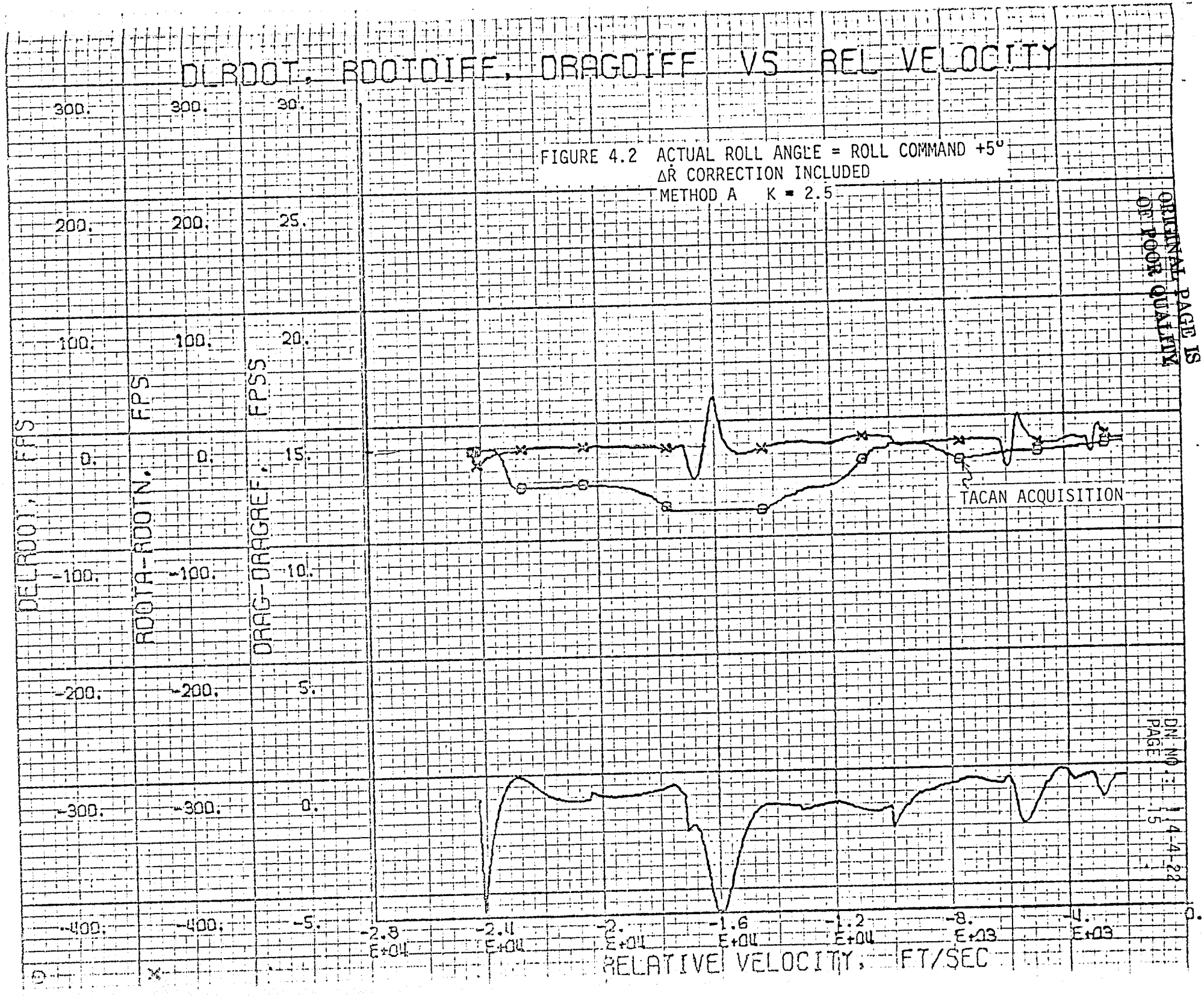

FIGURE 4.2 ACTUAL ROLL ANGLE = ROLL COMMAND +5°
$\Delta\dot{R}$ CORRECTION INCLUDED
METHOD A K = 2.5

4.0 RESULTS

A number of SVDS entry simulations have been run inputting the various error sources discussed previously. Representative results for both methods A and B for several error sources are presented in figure sets 5 through 9. The first three figures of each set, for example Figures 5.1, 5.2, and 5.3, show the study case with no $\Delta\dot{R}$ correction applied, i.e., using current ADC guidance. The first figure of each set, for example Figure 5.1, shows the reference drag and actual drag profile for each case. The second figure, example Figure 5.2, shows the vehicle roll history and azimuth error as a function of relative velocity for this case. The third figure, example Figure 5.3, shows the $\Delta\dot{R}$ correction incorporated into the guidance controller equation. This figure also shows the navigated altitude rate error ($\dot{R}$ actual - $\dot{R}$ navigated), and ($D-D_r$) values as functions of relative velocity. The next three figures of each set, for example Figures 5.4, 5.5, and 5.6, show the same plots respectively for that error source using integration method A. The next three figures of each set, for example, Figures 5.7, 5.8, and 5.9, show results of integration method B. Table I lists the cases presented in these figures. A brief discussion of these cases follows.

Figure 5 shows the nominal trajectory number 60412 SVDS simulation results with no errors input. All cases included in this section use the current standard roll attitude dead band of $\pm 3°$, which causes the drag bias in Figure 5.1. Figures 5.4 and 5.7 show the nominal trajectory drag-velocity profiles with the two drag feedback

methods. For this case very little $\Delta\dot{R}$ correction is applied.

Figure 6.1 shows the drag bias for the uncorrected guidance case with a platform pitch misalignment of +.46° at entry interface (≈6σ error, Reference C). This misalignment causes a drag bias of up to 3.5 feet per second-squared, equivalent to an error of approximately 120 feet per second in the navigated altitude rate (Figure 6.3). Both integration methods A and B of calculating $\Delta\dot{R}$ enabled the drag to follow the reference drag better as presented in Figures 6.4 - 6.9. Figure set 7 presents the results of inputting a negative pitch misalignment of the same magnitude. The corrected-guidance results of this -.46° pitch misalignment case are presented in Figure 7.4 - 7.9. Again both correction methods performed adequately.

Figure 8.1 shows the drag bias for the uncorrected guidance case with combined errors of +.46° platform pitch misalignment, 3σ headwind and 3σ low L/D aerodynamics. Both integration methods enabled the drag to more closely follow the reference as shown in Figures 8.4 - 8.9. Figure set 9 presents results of combined errors of -.46° pitch misalignment, 3σ tailwind, and 3σ high L/D aerodynamics and, again, both correction methods produced adequate performance.

TABLE I

LIST OF STUDY CASES PRESENTED

Figures 5.1 - 5.9	Nominal Trajectory Number 60412 (OFT-1) No Errors
Figures 6.1 - 6.9	Platform Pitch Misalignment +.46° at Entry Interface
Figures 7.1 - 7.9	Platform Pitch Misalignment -.46° at Entry Interface
Figures 8.1 - 8.9	Combined Error Case Platform Pitch Misalignment = +.46° 3σ Headwind 3σ Low L/D (SVDS Aerodynamic Dispersion Study Point 6)
Figures 9.1 - 9.9	Combined Error Case Platform Pitch Misalignment = -.46° 3σ Tailwind 3σ High L/D (SVDS Aerodynamic Dispersion Study Point 3)

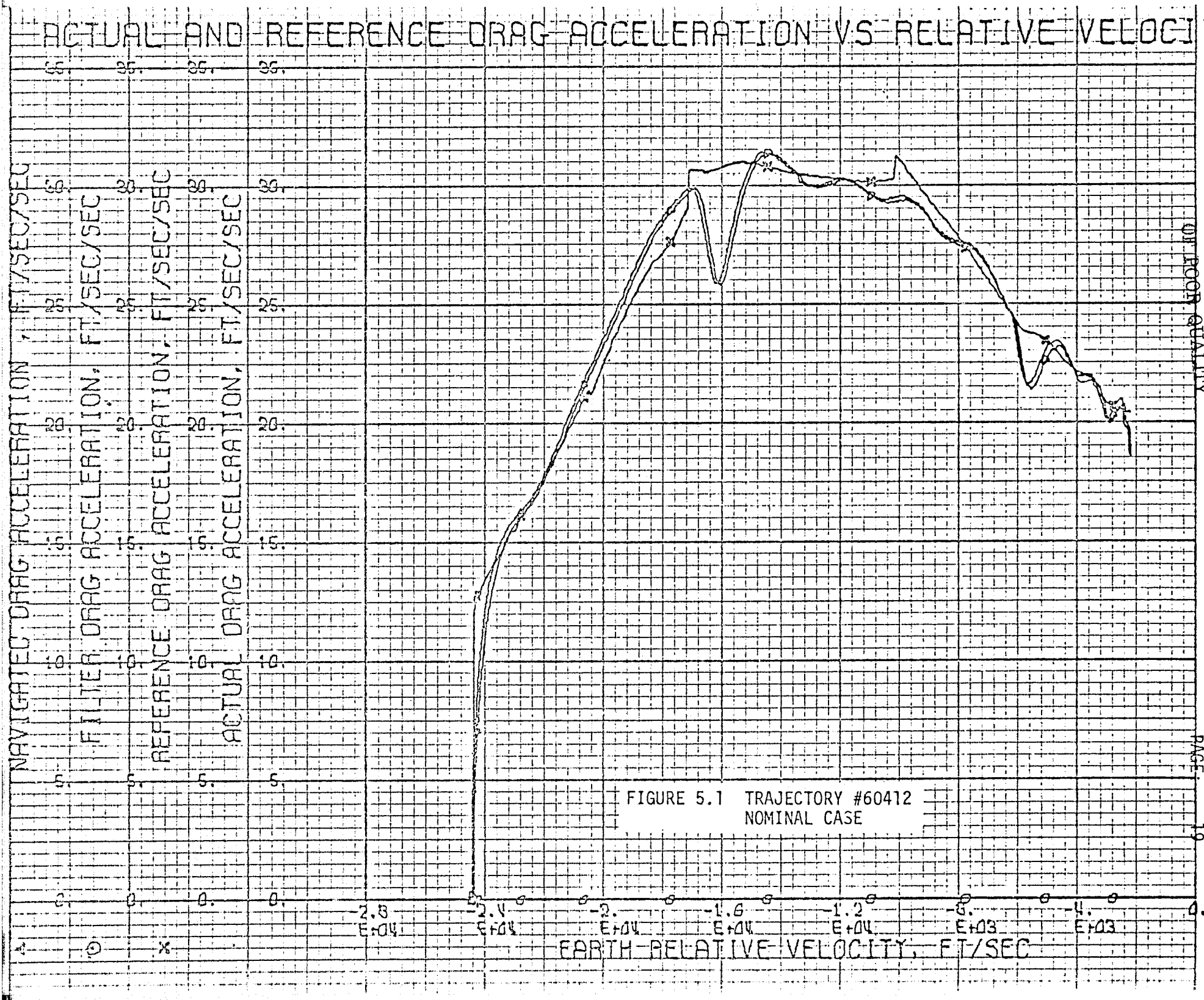

FIGURE 5.1 TRAJECTORY #60412
NOMINAL CASE

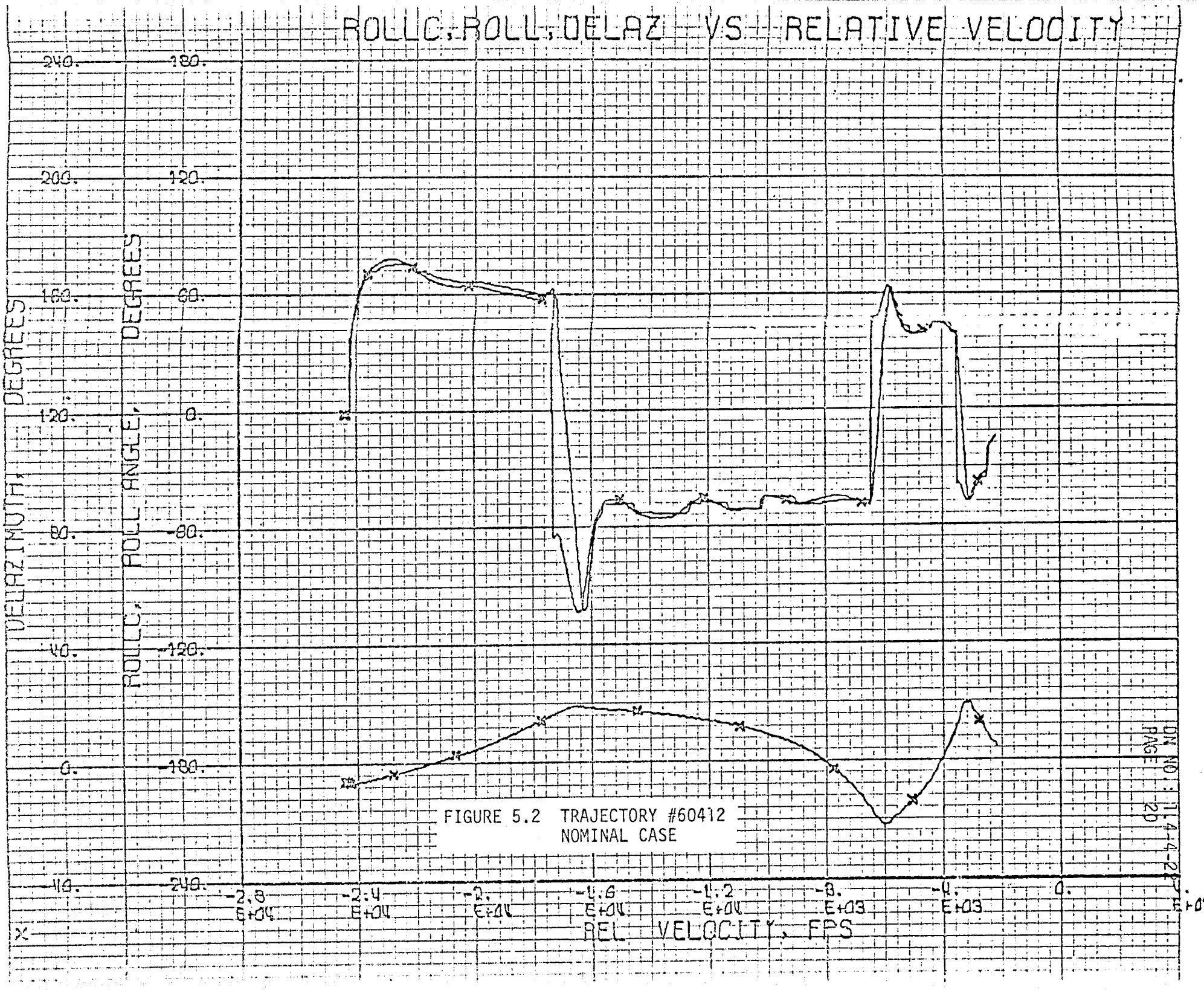

FIGURE 5.2 TRAJECTORY #60412
NOMINAL CASE

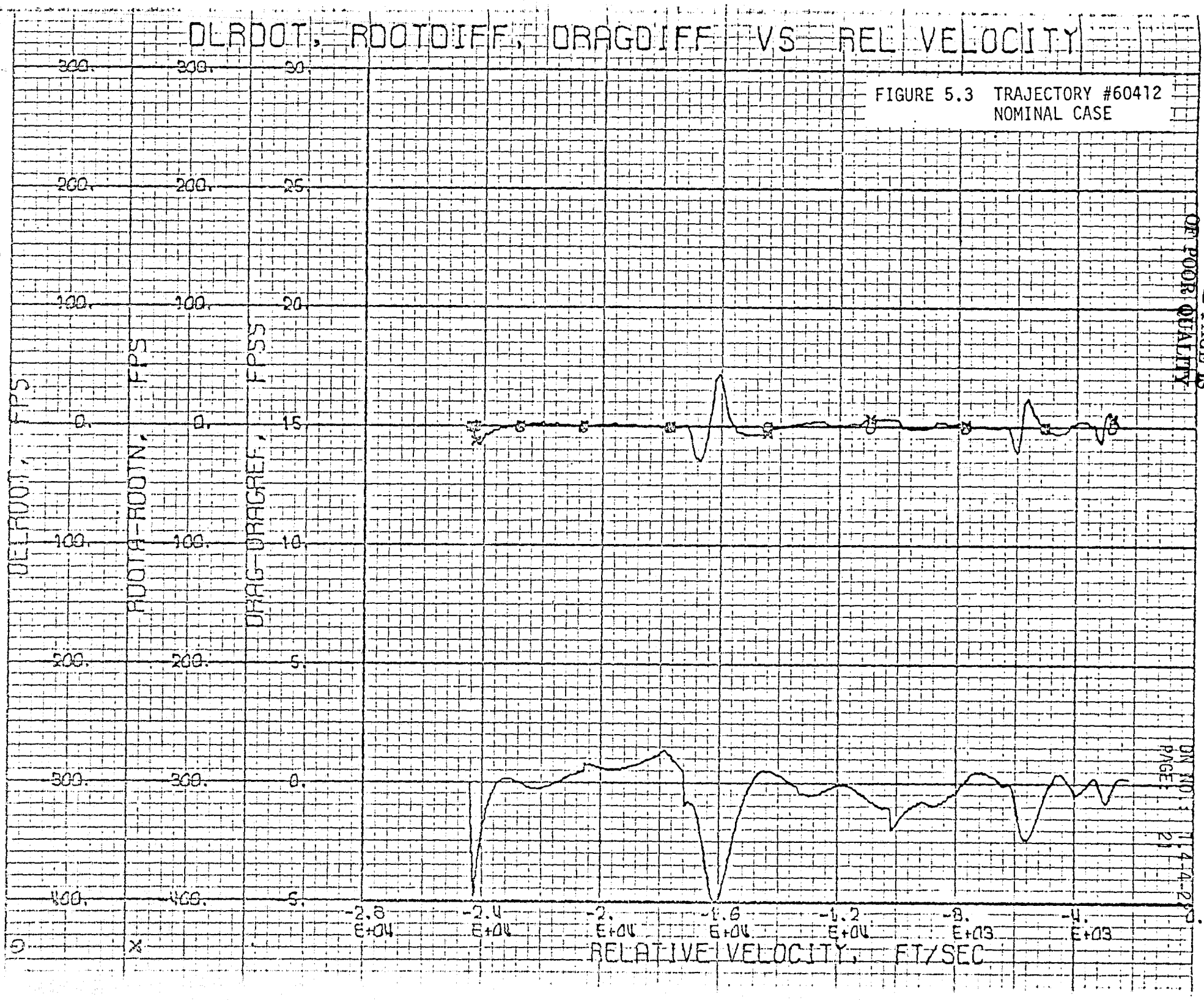

FIGURE 5.3 TRAJECTORY #60412
NOMINAL CASE

ORIGINAL PAGE IS
OF POOR QUALITY

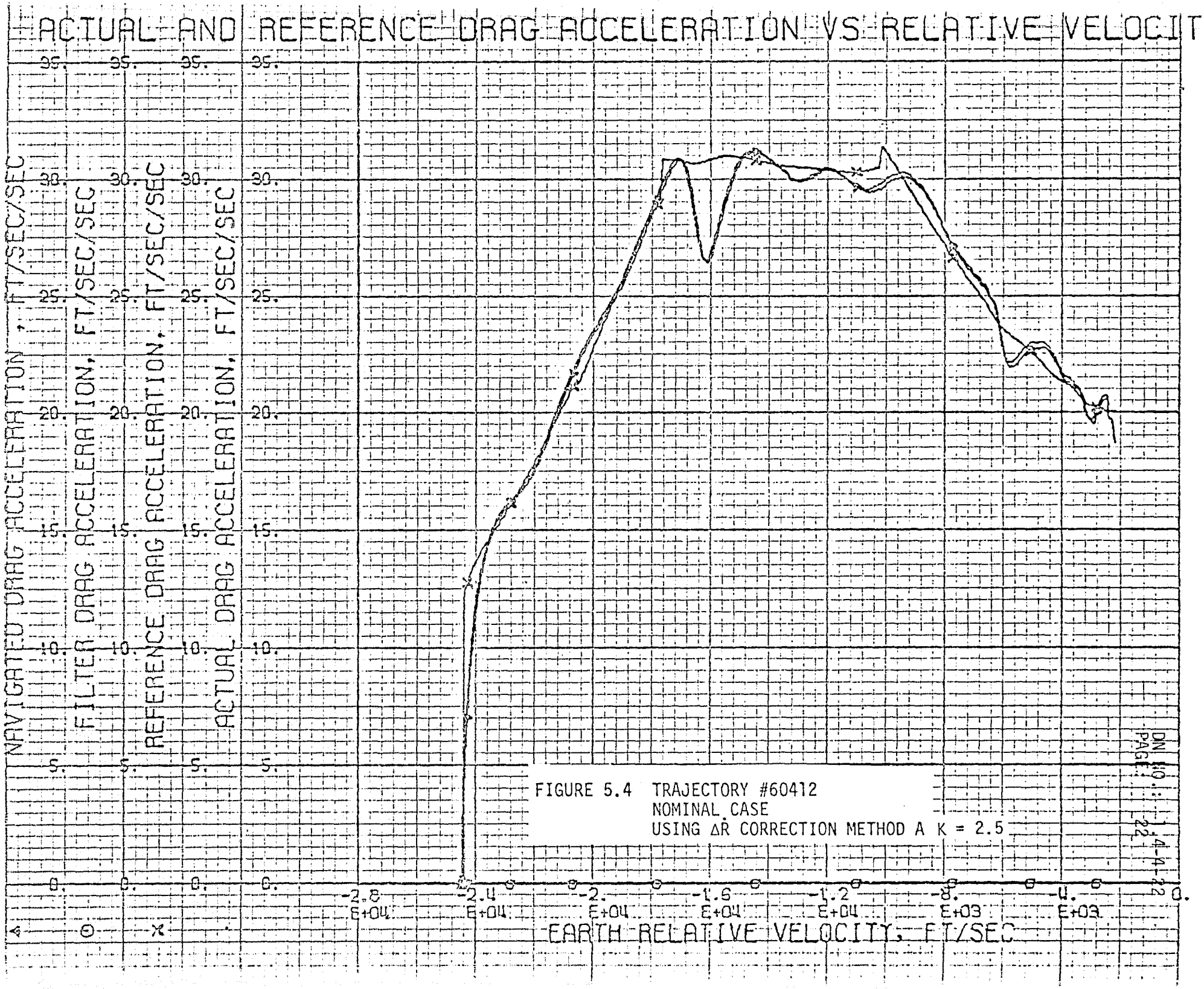

FIGURE 5.4 TRAJECTORY #60412
NOMINAL CASE
USING $\Delta\dot{R}$ CORRECTION METHOD A K = 2.5

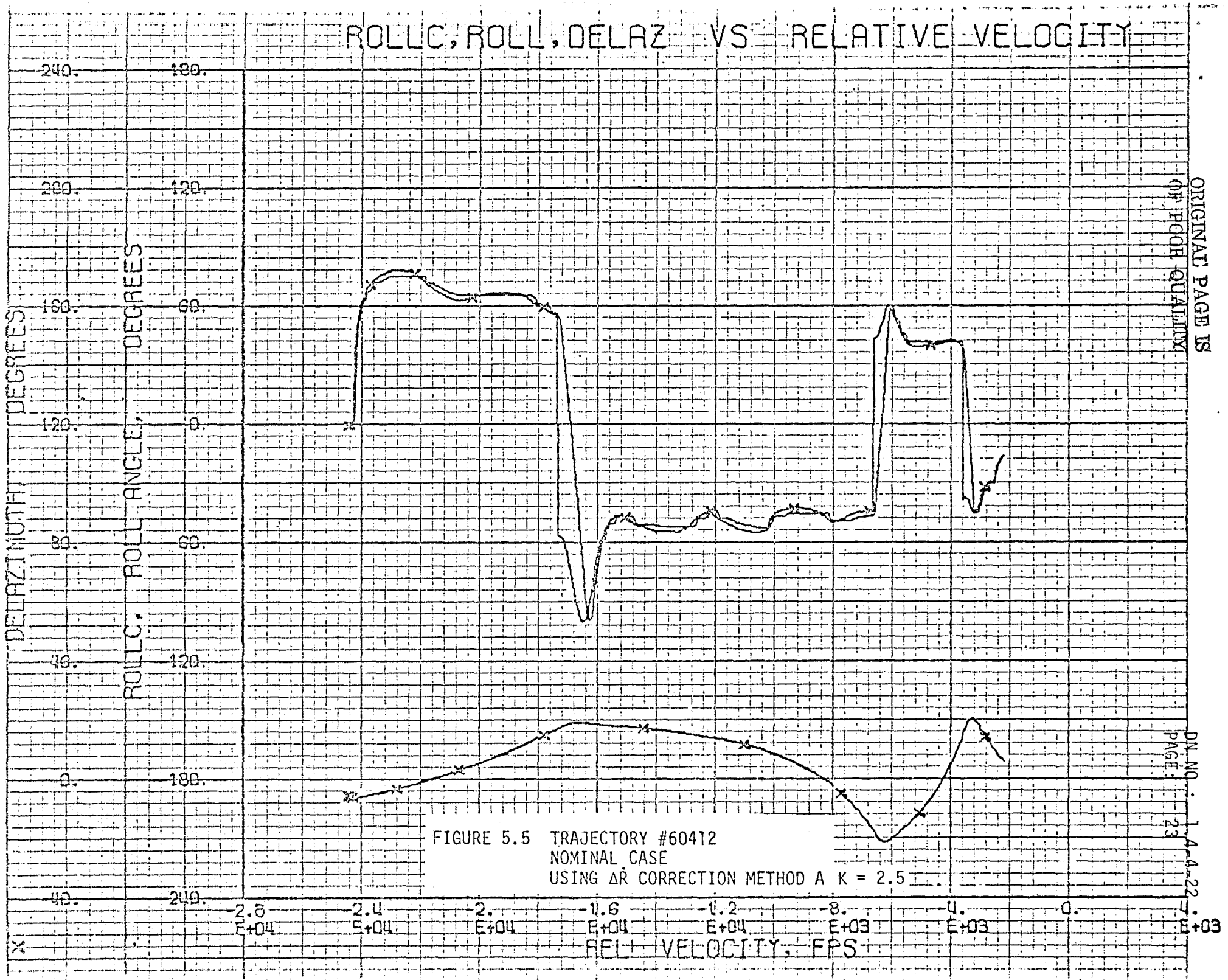

FIGURE 5.5 TRAJECTORY #60412
NOMINAL CASE
USING $\Delta\dot{R}$ CORRECTION METHOD A K = 2.5

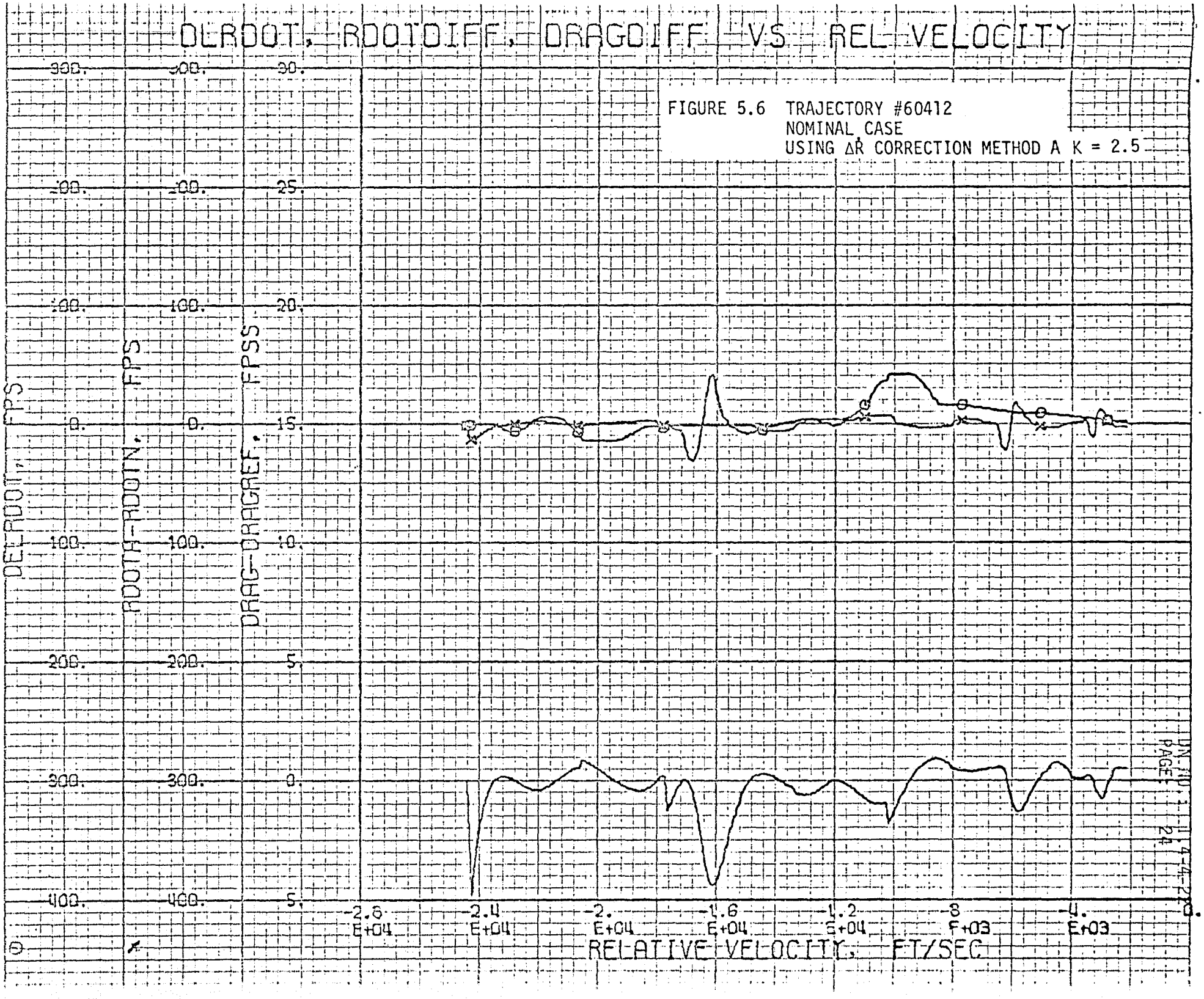

FIGURE 5.6 TRAJECTORY #60412
NOMINAL CASE
USING $\Delta\dot{R}$ CORRECTION METHOD A K = 2.5

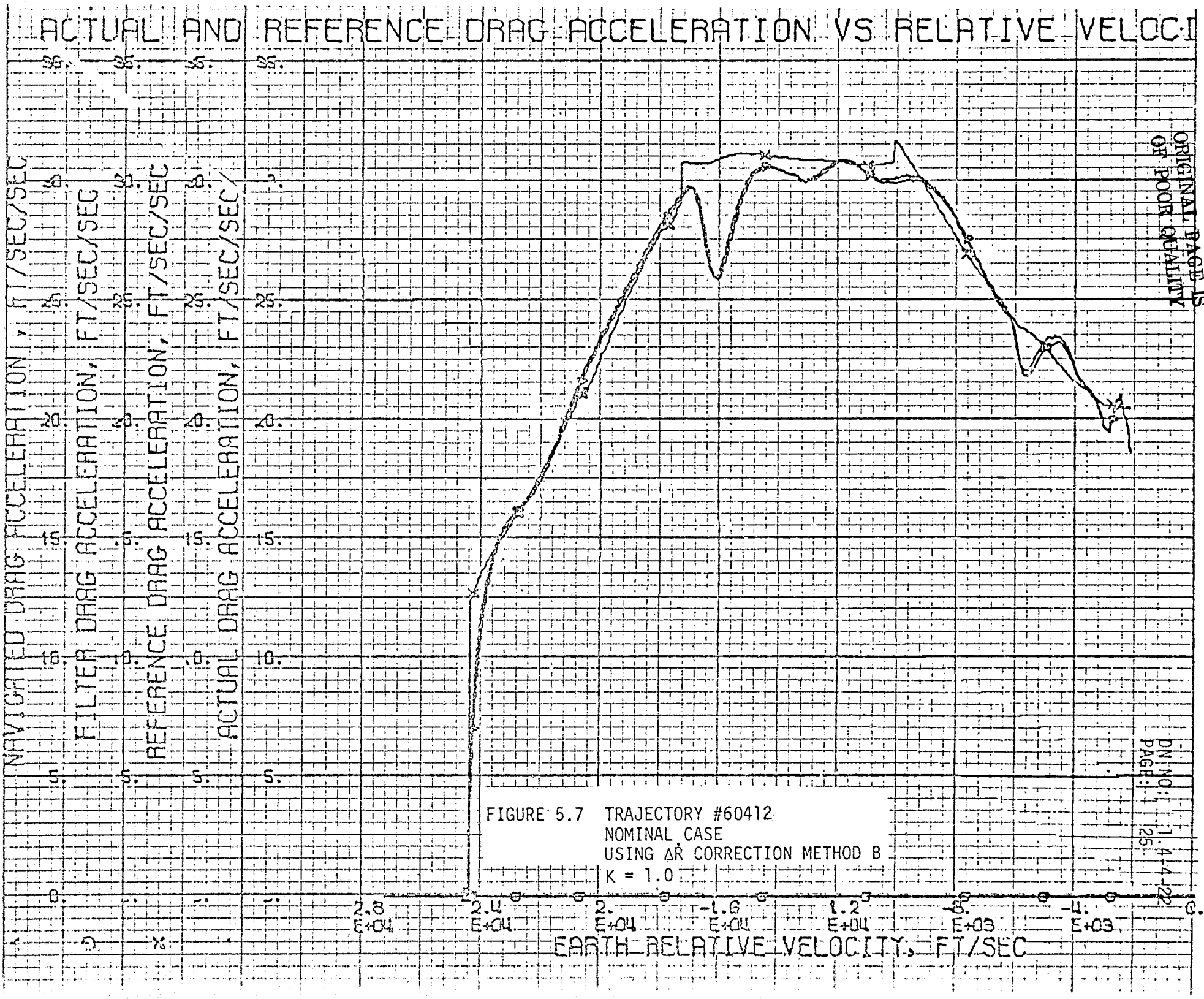

FIGURE 5.7 TRAJECTORY #60412
NOMINAL CASE
USING $\Delta\dot{R}$ CORRECTION METHOD B
K = 1.0

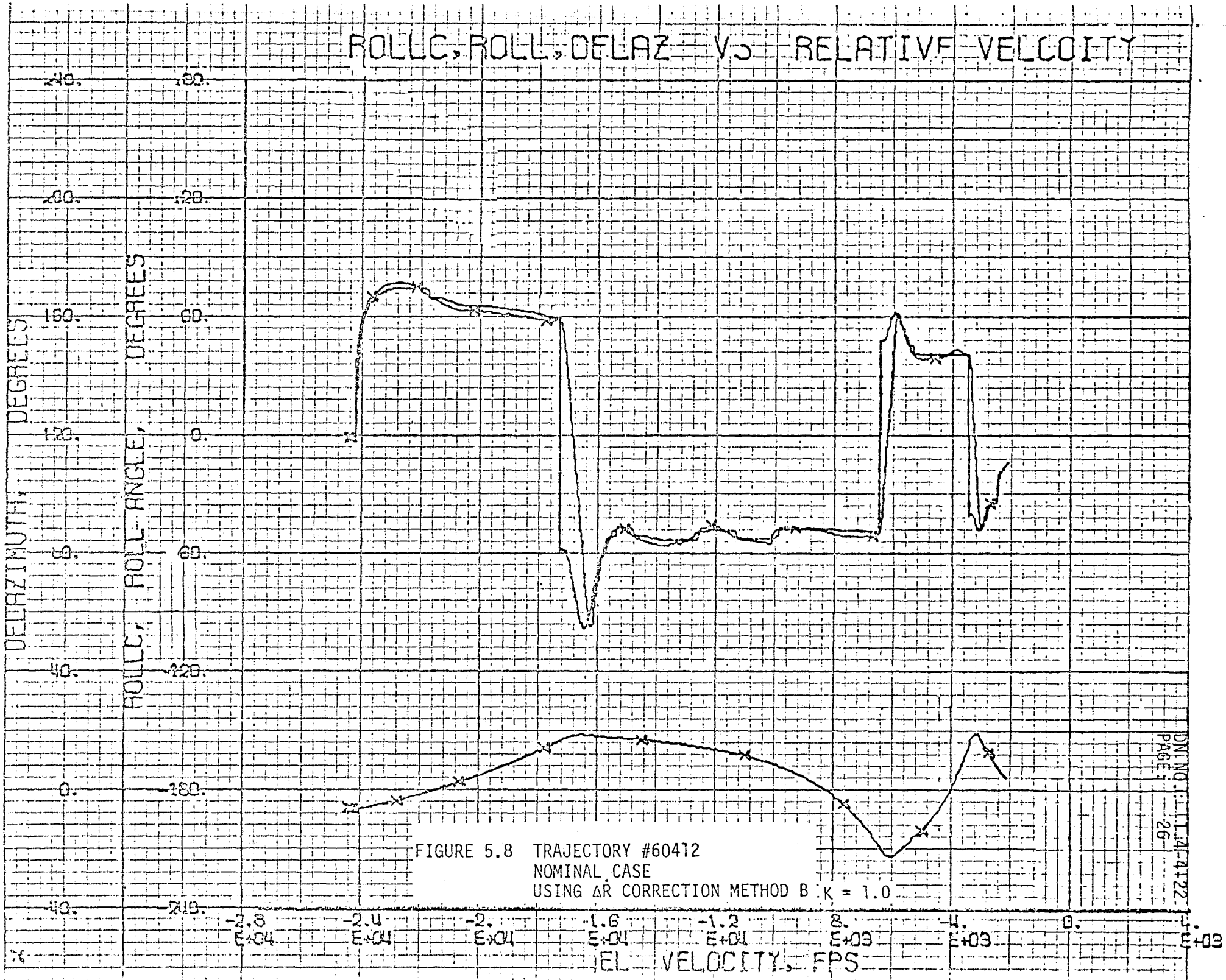

FIGURE 5.8 TRAJECTORY #60412
NOMINAL CASE
USING ΔR CORRECTION METHOD B K = 1.0

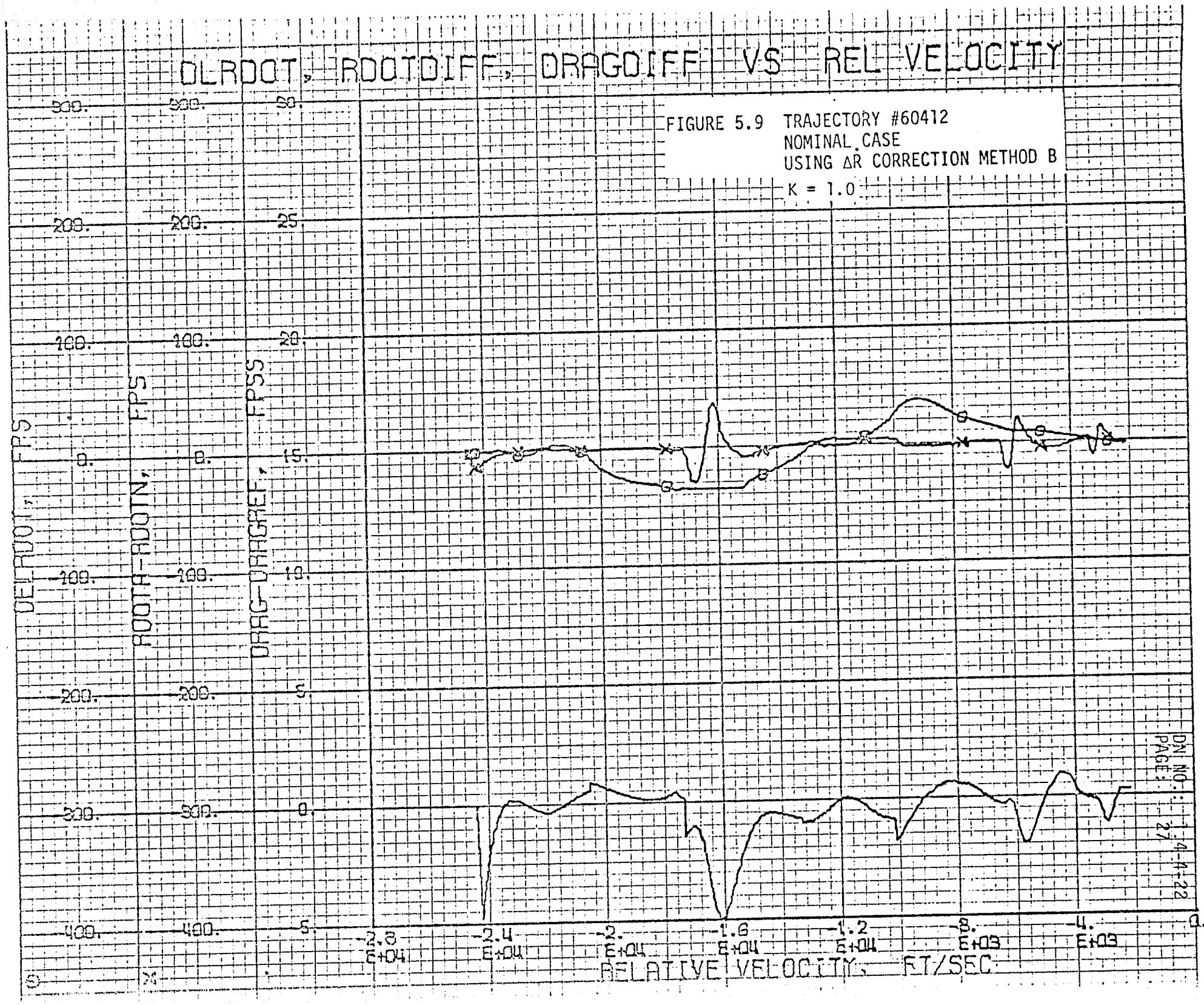
DLRDOT, RDOTDIFF, DRAGDIFF VS REL VELOCITY
FIGURE 5.9 TRAJECTORY #60412
NOMINAL CASE
USING ΔR CORRECTION METHOD B
K = 1.0
DLRDOT, FPS
RDOTR-RDOTN, FPS
DRAG-DRAGREF, FPSS
300.
200.
100.
0.
-100.
-200.
-300.
-400.
50.
25.
20.
15.
10.
5.
0.
-5.
-2.8 E+04
-2.4 E+04
-2. E+04
-1.6 E+04
-1.2 E+04
-8. E+03
-4. E+03
0.
RELATIVE VELOCITY, FT/SEC
DN NO.: 1-4-4-22
PAGE: 27

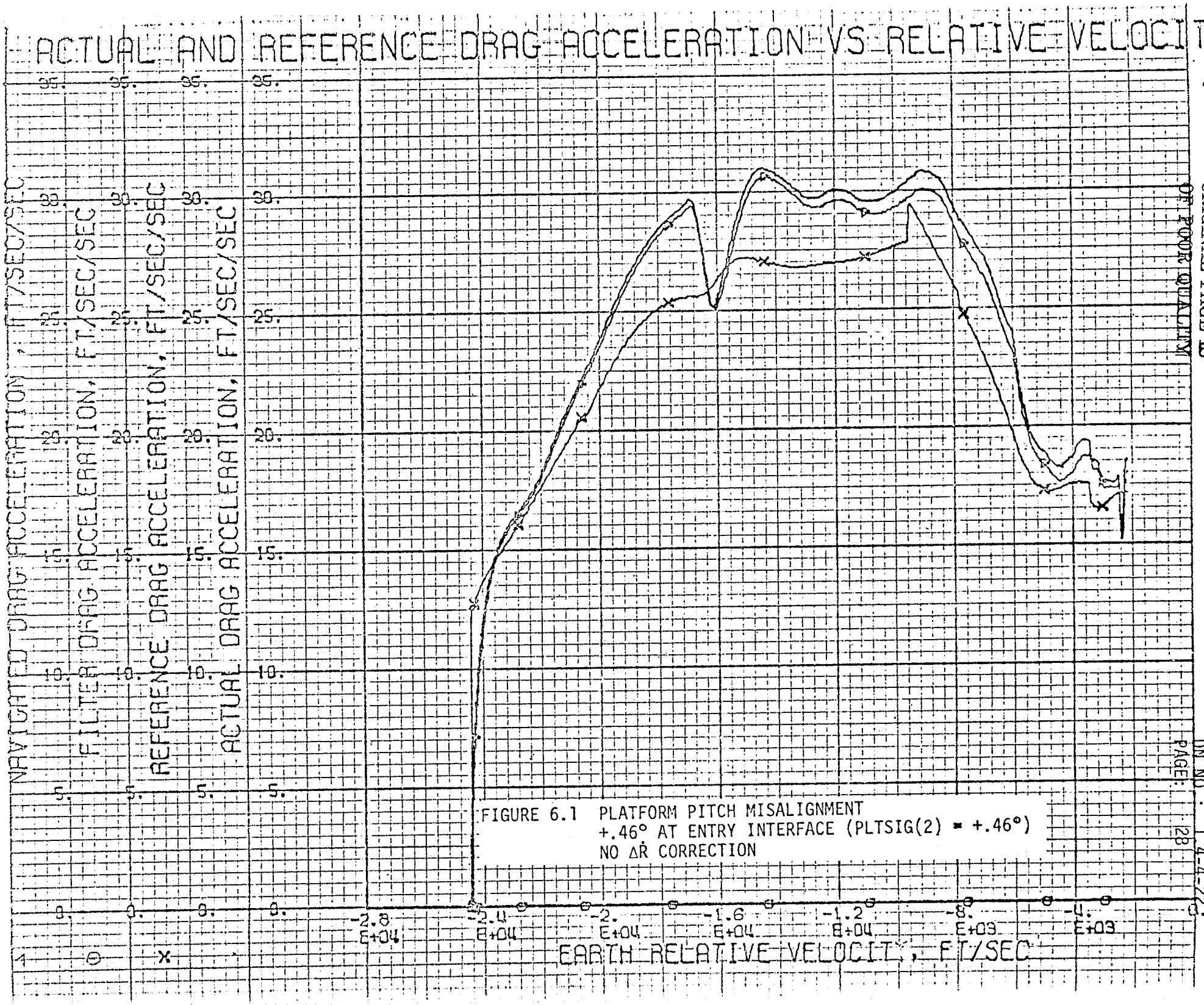

FIGURE 6.1 PLATFORM PITCH MISALIGNMENT
+.46° AT ENTRY INTERFACE (PLTSIG(2) = +.46°)
NO $\Delta\dot{R}$ CORRECTION

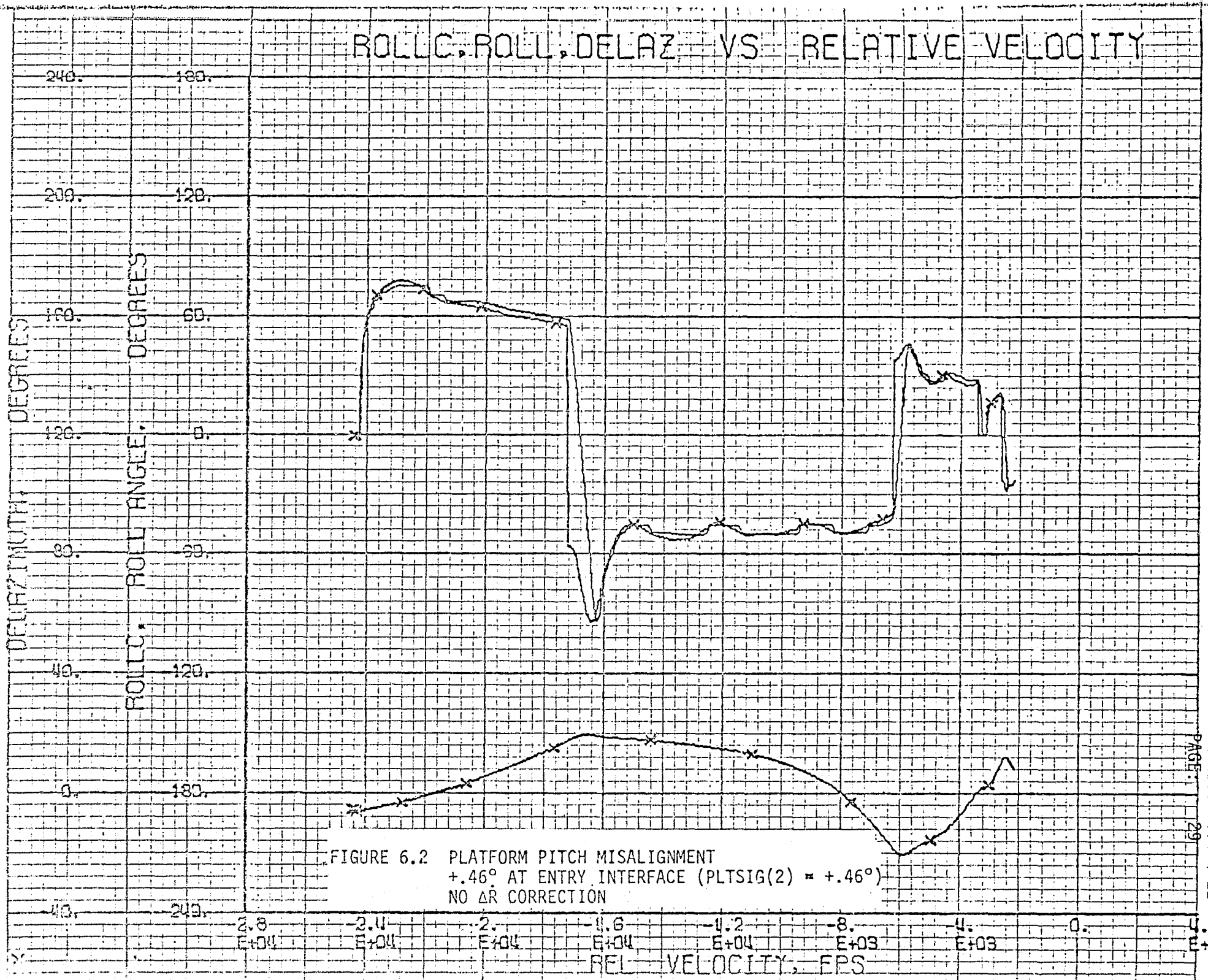

FIGURE 6.2 PLATFORM PITCH MISALIGNMENT
+.46° AT ENTRY INTERFACE (PLTSIG(2) = +.46°)
NO ΔR CORRECTION

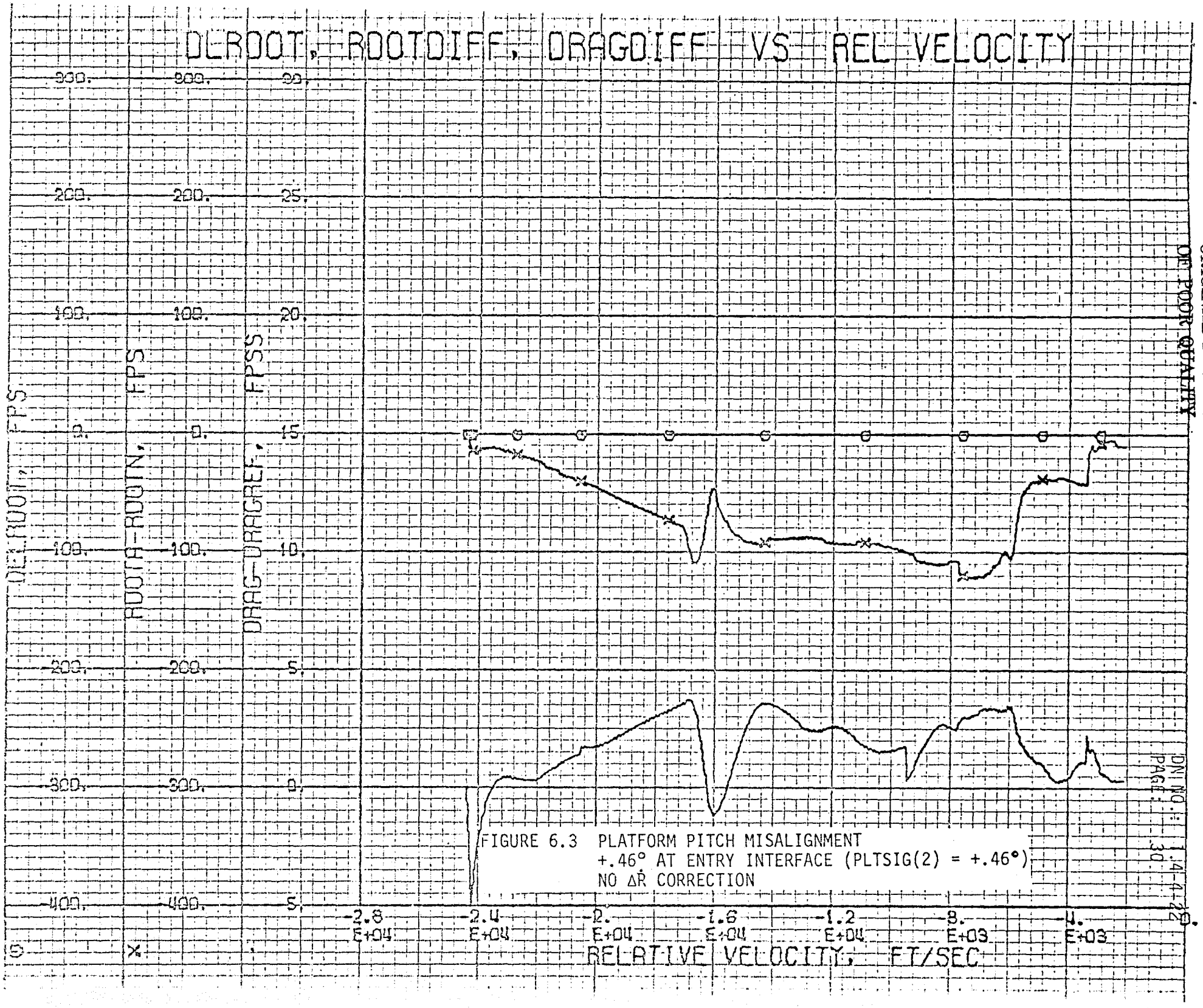

FIGURE 6.3 PLATFORM PITCH MISALIGNMENT
+.46° AT ENTRY INTERFACE (PLTSIG(2) = +.46°)
NO $\Delta\dot{R}$ CORRECTION

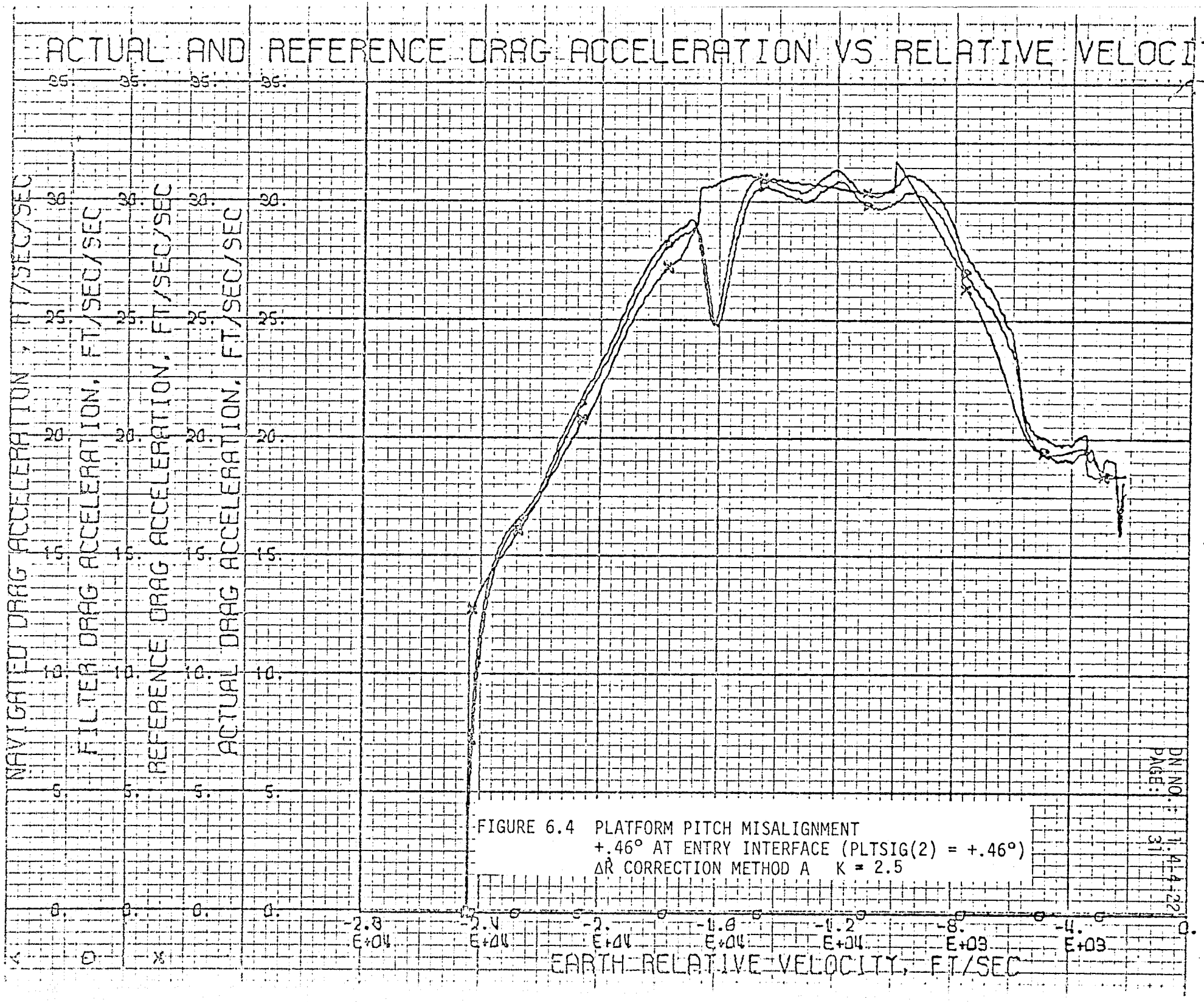

FIGURE 6.4 PLATFORM PITCH MISALIGNMENT
+.46° AT ENTRY INTERFACE (PLTSIG(2) = +.46°)
$\Delta\dot{R}$ CORRECTION METHOD A K = 2.5

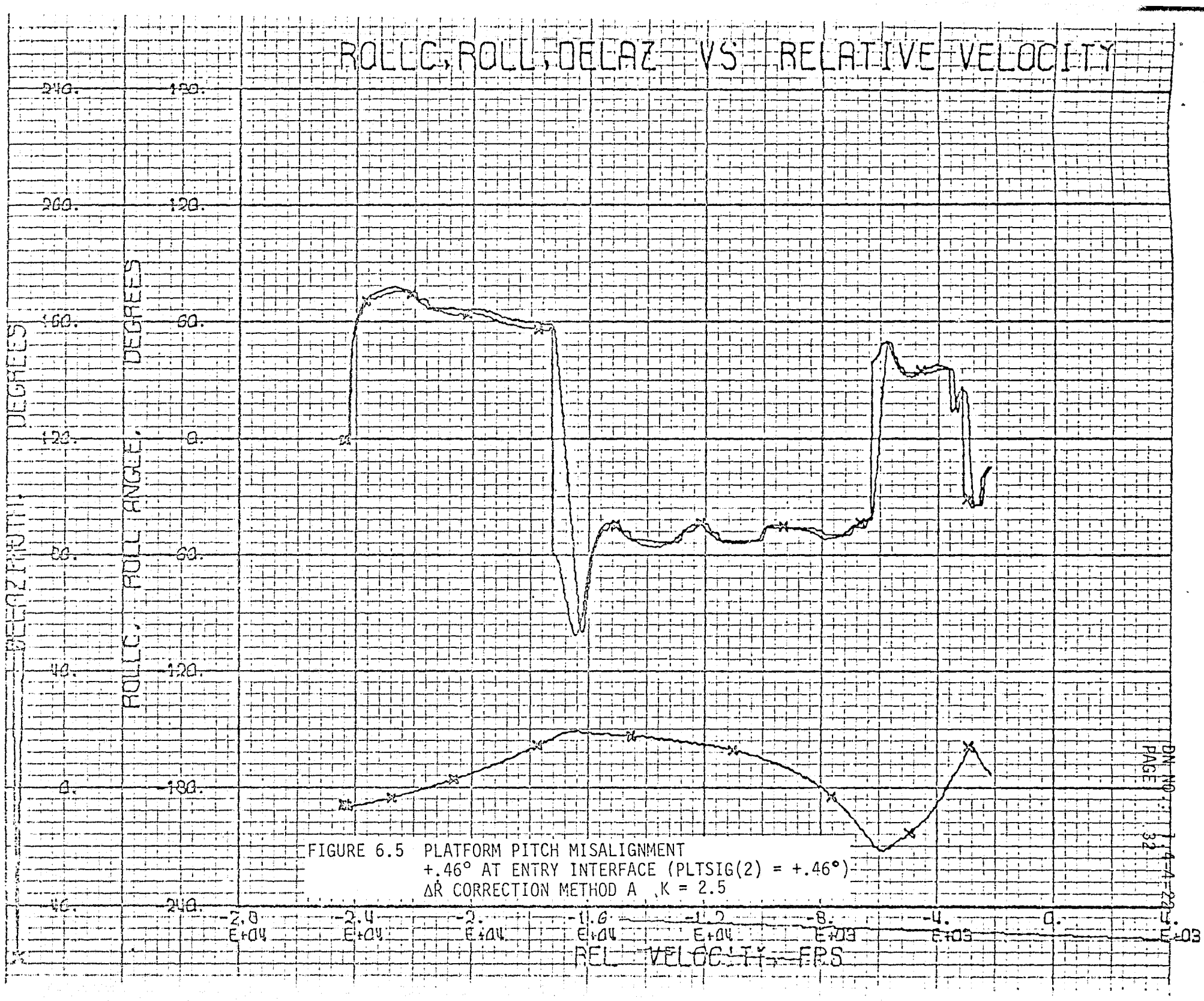

FIGURE 6.5 PLATFORM PITCH MISALIGNMENT
+.46° AT ENTRY INTERFACE (PLTSIG(2) = +.46°)
$\Delta\dot{R}$ CORRECTION METHOD A , K = 2.5

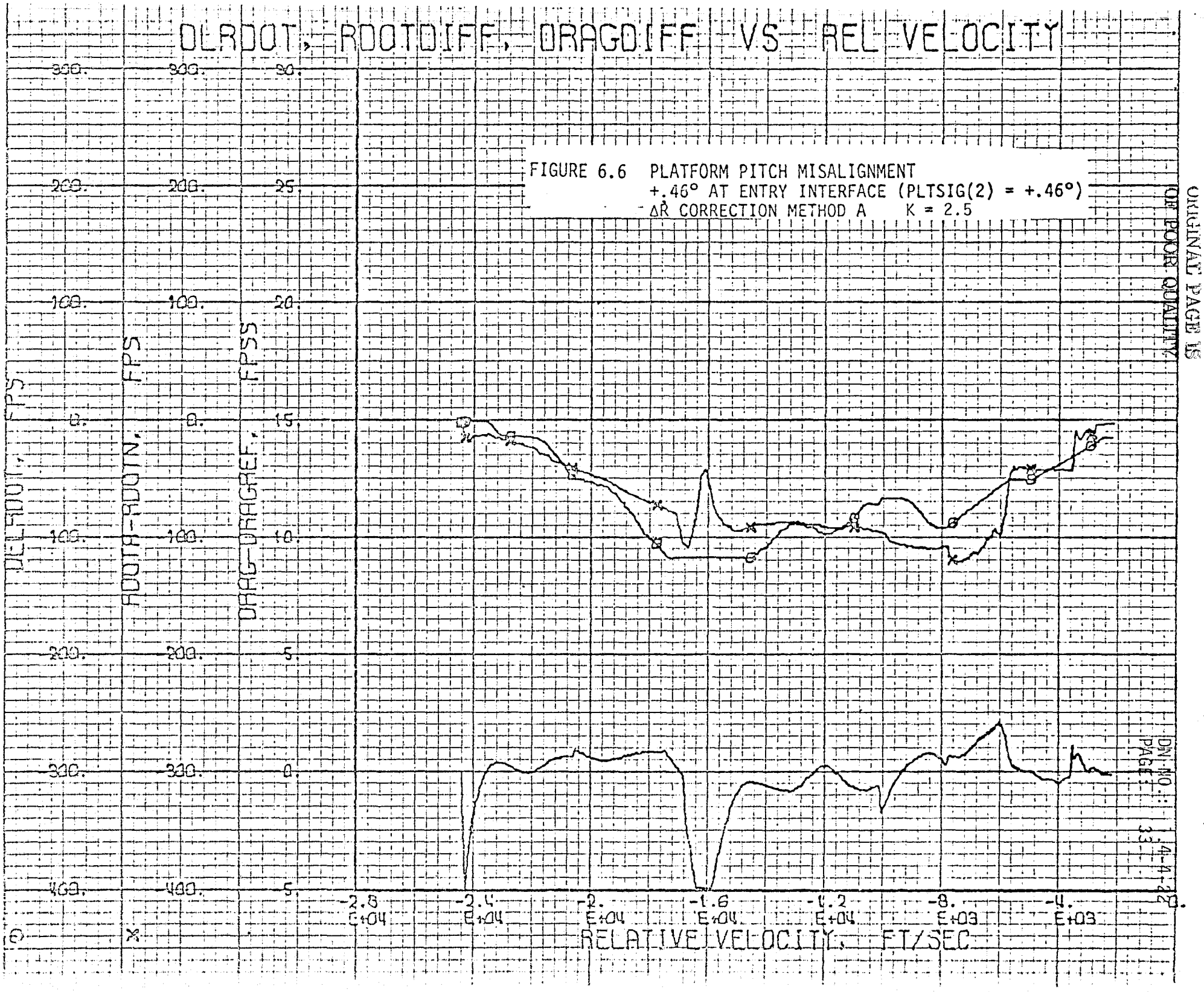

FIGURE 6.6 PLATFORM PITCH MISALIGNMENT
+.46° AT ENTRY INTERFACE (PLTSIG(2) = +.46°)
$\Delta\dot{R}$ CORRECTION METHOD A K = 2.5

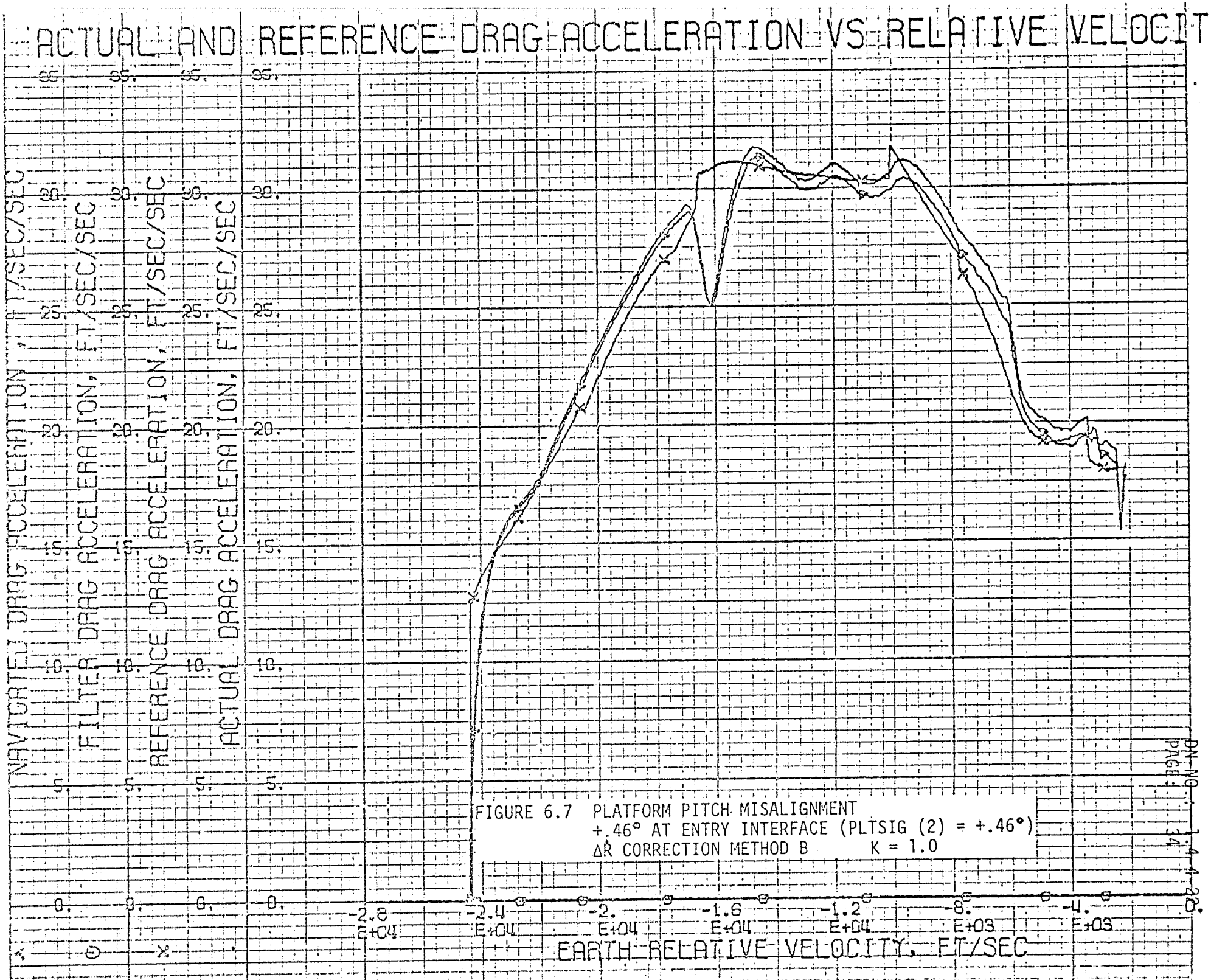

FIGURE 6.7 PLATFORM PITCH MISALIGNMENT
+.46° AT ENTRY INTERFACE (PLTSIG (2) = +.46°)
$\Delta\hat{R}$ CORRECTION METHOD B K = 1.0

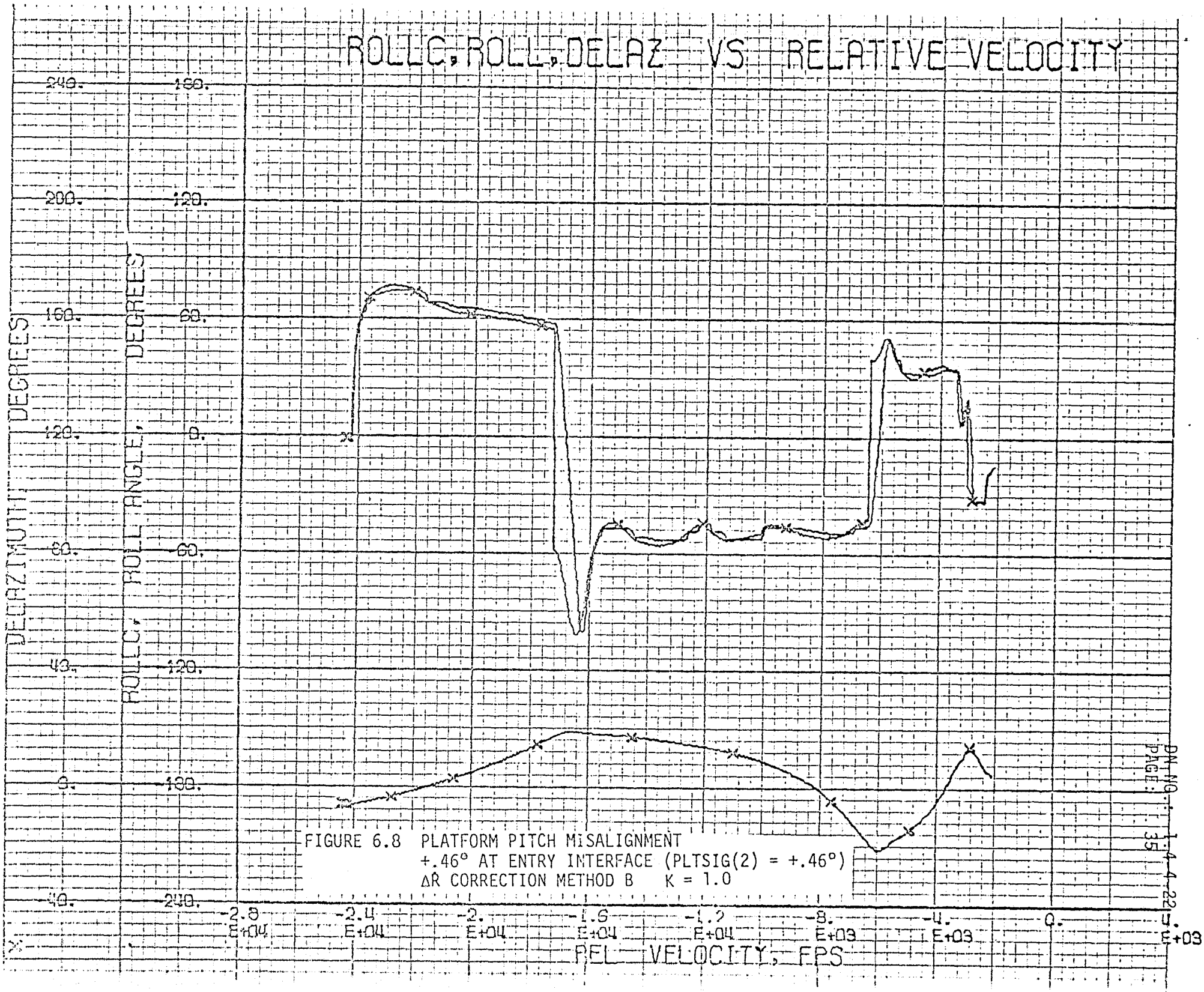

FIGURE 6.8 PLATFORM PITCH MISALIGNMENT
+.46° AT ENTRY INTERFACE (PLTSIG(2) = +.46°)
ΔR CORRECTION METHOD B K = 1.0

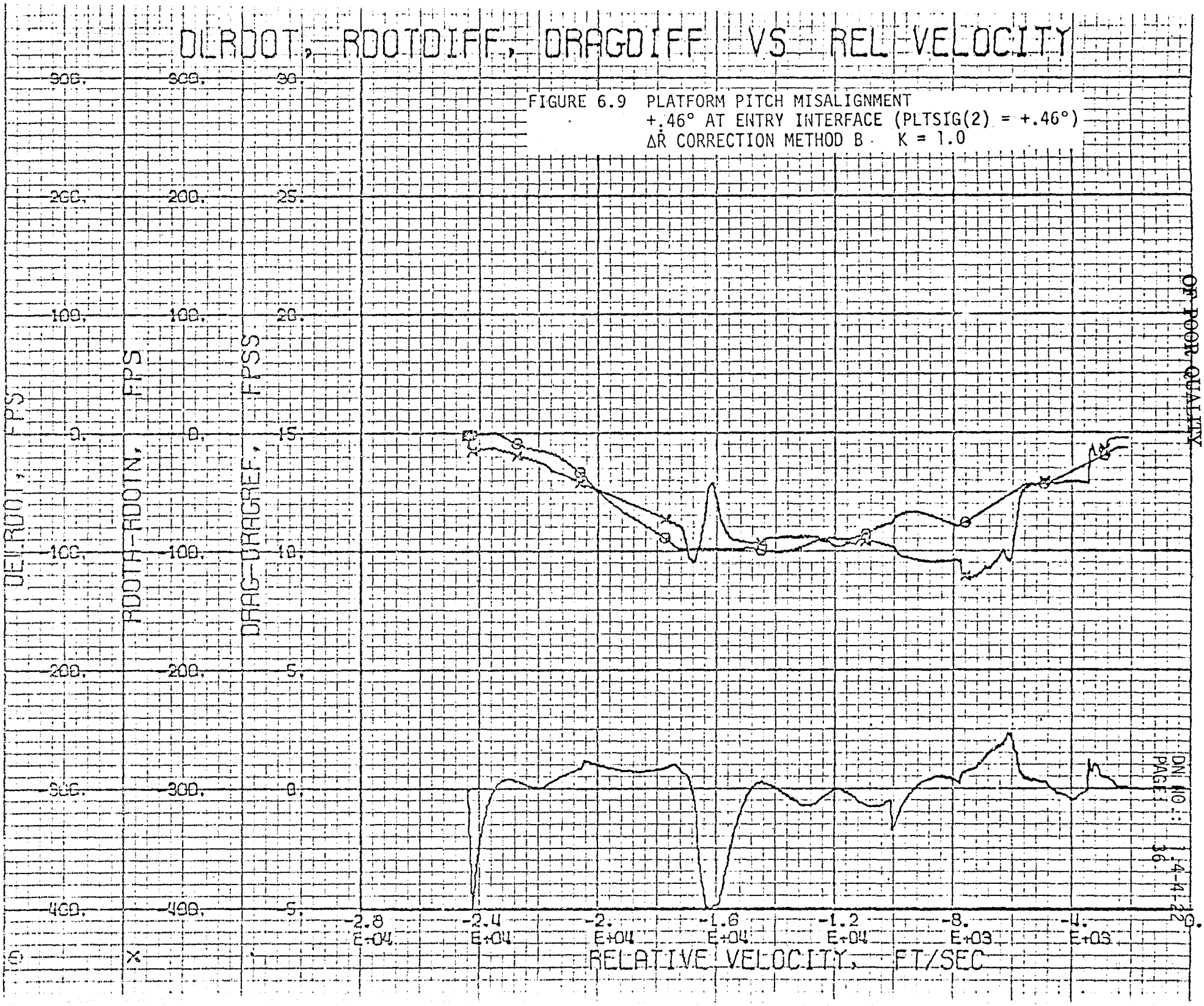

FIGURE 6.9 PLATFORM PITCH MISALIGNMENT
+.46° AT ENTRY INTERFACE (PLTSIG(2) = +.46°)
ΔR CORRECTION METHOD B K = 1.0

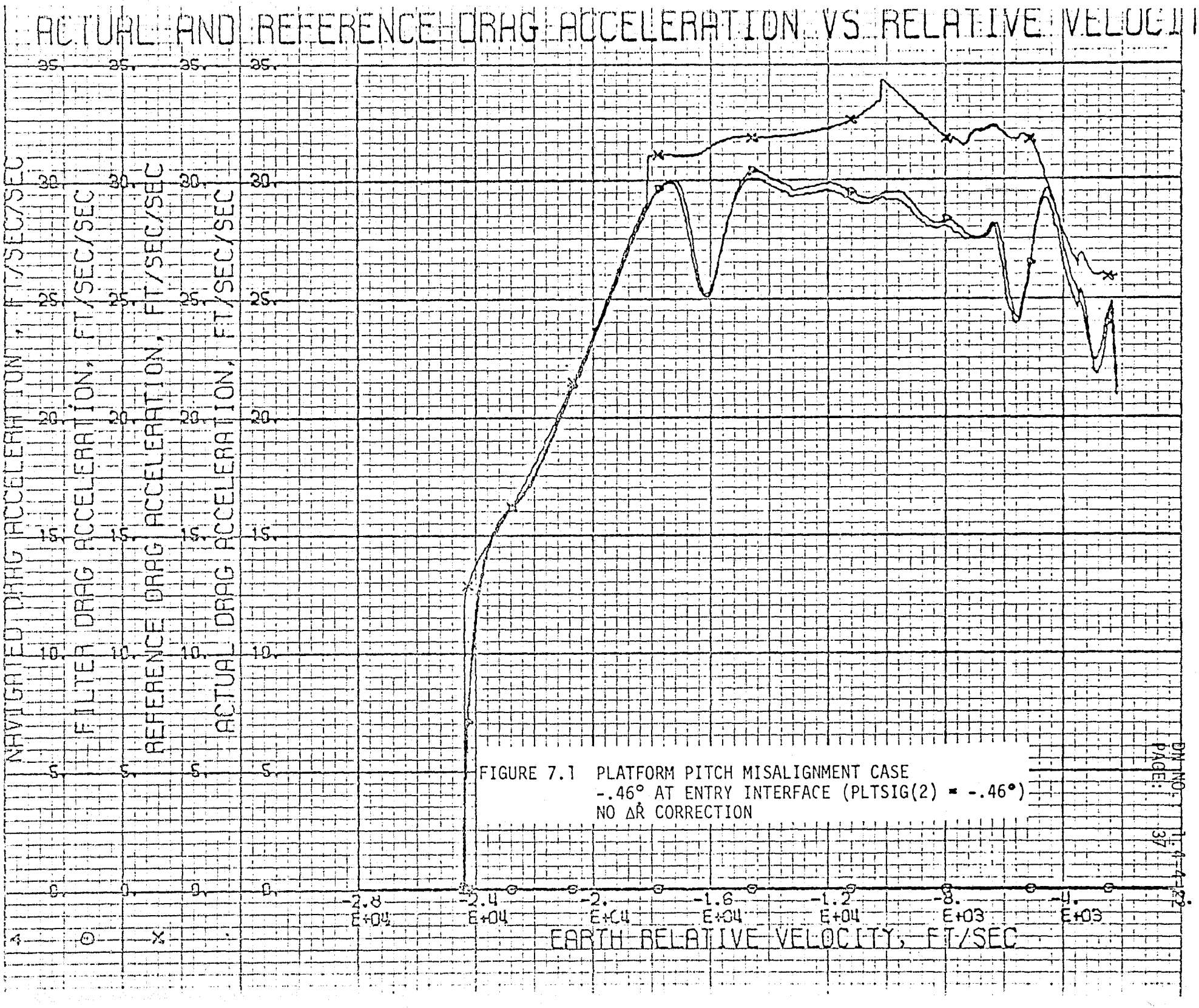

FIGURE 7.1 PLATFORM PITCH MISALIGNMENT CASE
-.46° AT ENTRY INTERFACE (PLTSIG(2) = -.46°)
NO $\Delta\dot{R}$ CORRECTION

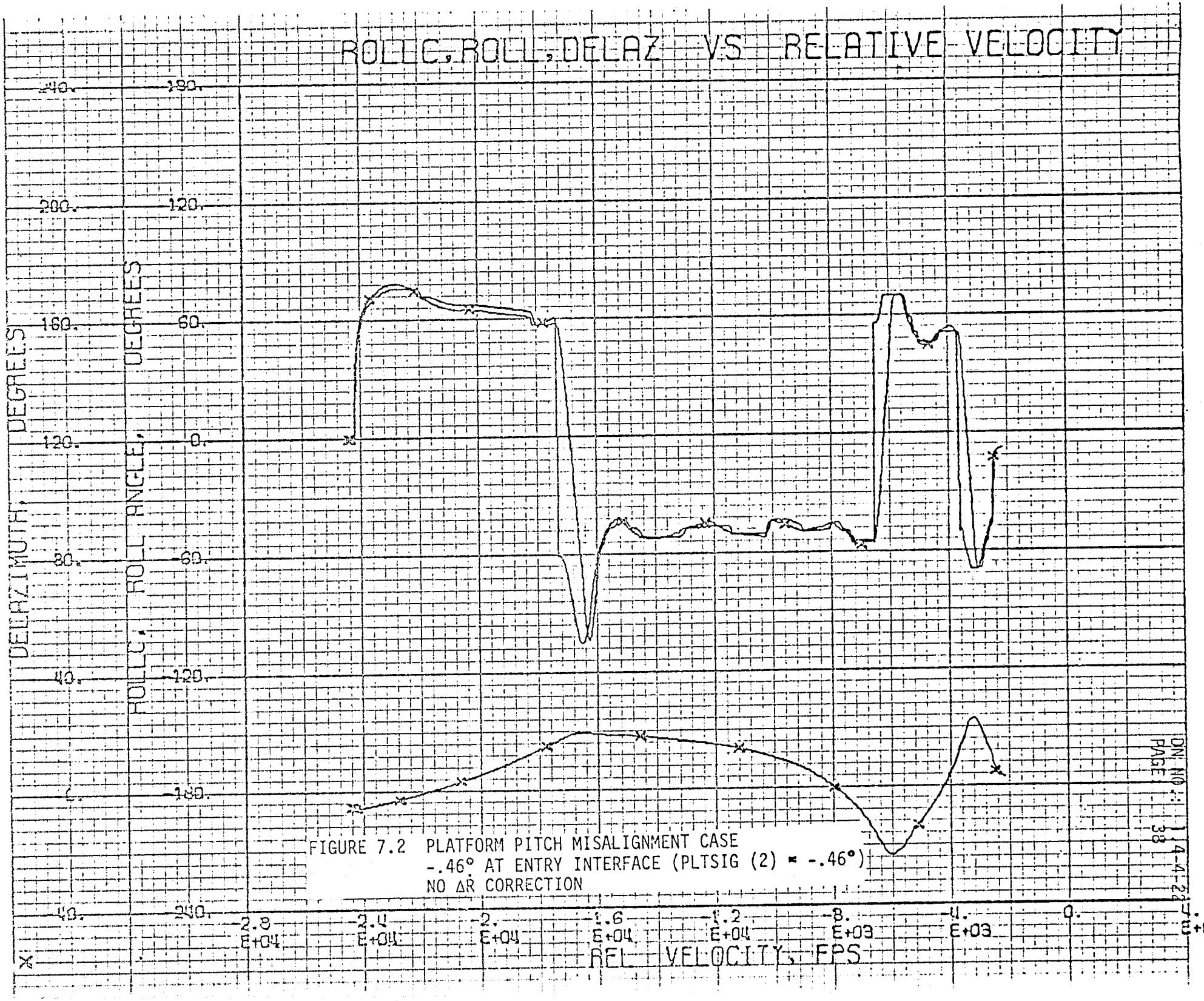

FIGURE 7.2 PLATFORM PITCH MISALIGNMENT CASE
-.46° AT ENTRY INTERFACE (PLTSIG (2) = -.46°)
NO ΔR CORRECTION

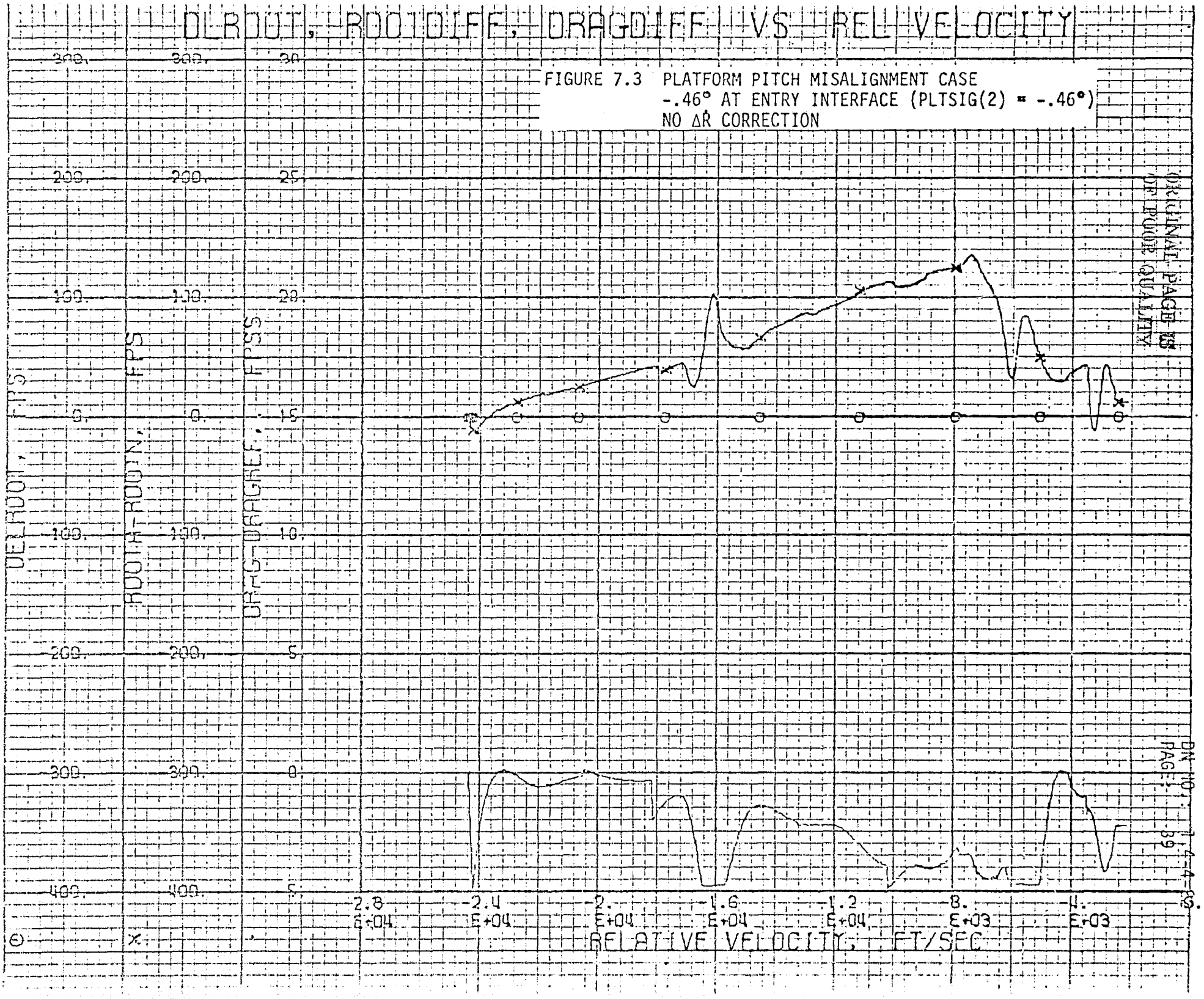
DLRDOT, ROOTDIFF, DRAGDIFF VS REL VELOCITY
FIGURE 7.3 PLATFORM PITCH MISALIGNMENT CASE
-.46° AT ENTRY INTERFACE (PLTSIG(2) = -.46°)
NO ΔR CORRECTION
DLRDOT, FPS
ROOTH-ROOTN, FPS
DRAG-DRAGREF, FPSS
300.
200.
100.
0.
100.
200.
300.
400.
30
25
20
15
10
5
0
5
-2.8 E+04
-2.4 E+04
-2. E+04
-1.6 E+04
-1.2 E+04
-8. E+03
-4. E+03
RELATIVE VELOCITY, FT/SEC
ORIGINAL PAGE IS OF POOR QUALITY
BN NO. 1-4-69
PAGE 89

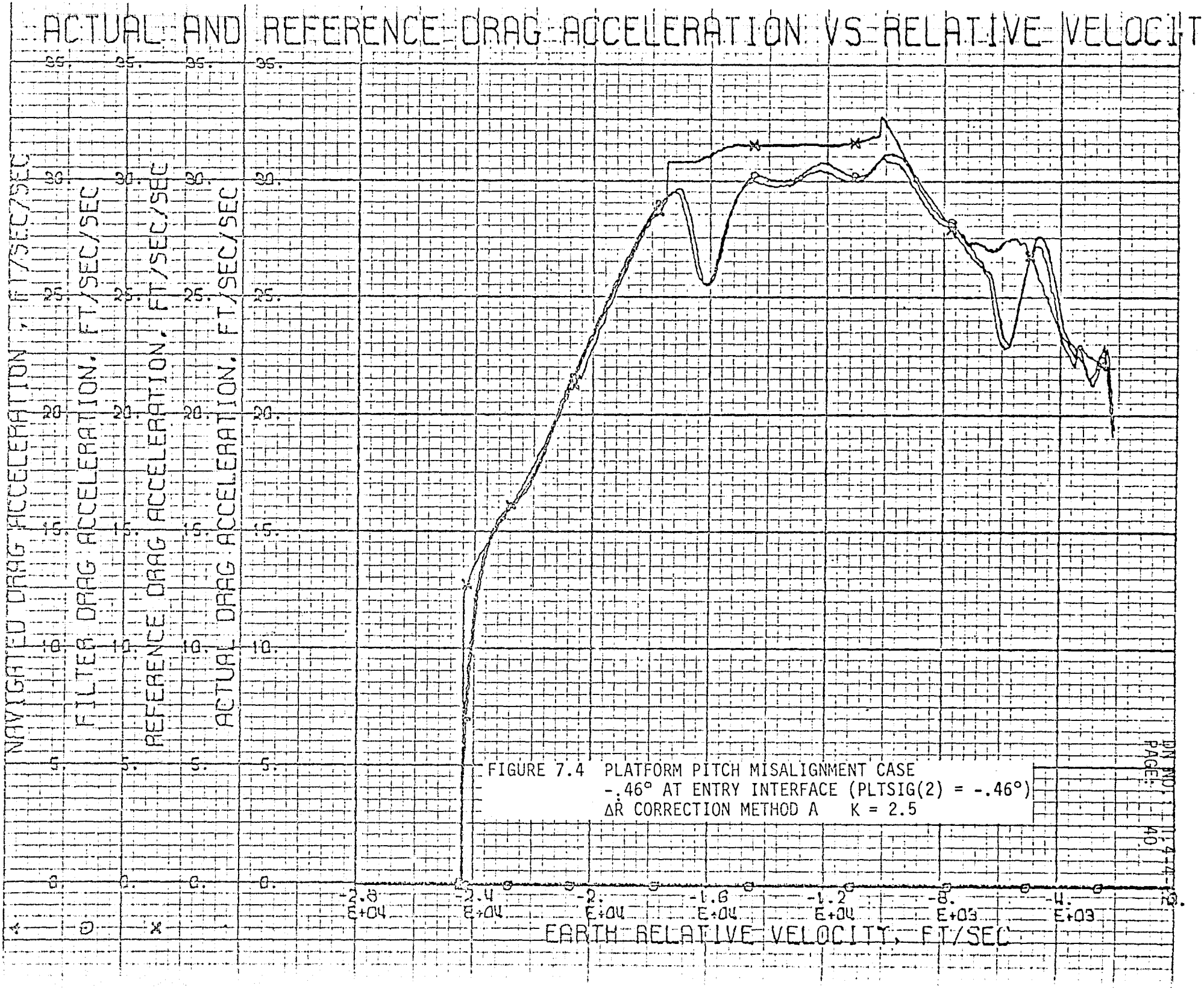

FIGURE 7.4 PLATFORM PITCH MISALIGNMENT CASE
-.46° AT ENTRY INTERFACE (PLTSIG(2) = -.46°)
$\Delta\dot{R}$ CORRECTION METHOD A K = 2.5

FIGURE 7.5 PLATFORM PITCH MISALIGNMENT CASE
-.46° AT ENTRY INTERFACE (PLTSIG(2) = -.46°)
$\Delta\dot{R}$ CORRECTION METHOD A K = 2.5

ON NO. 1 4-4-2
PAGE 41

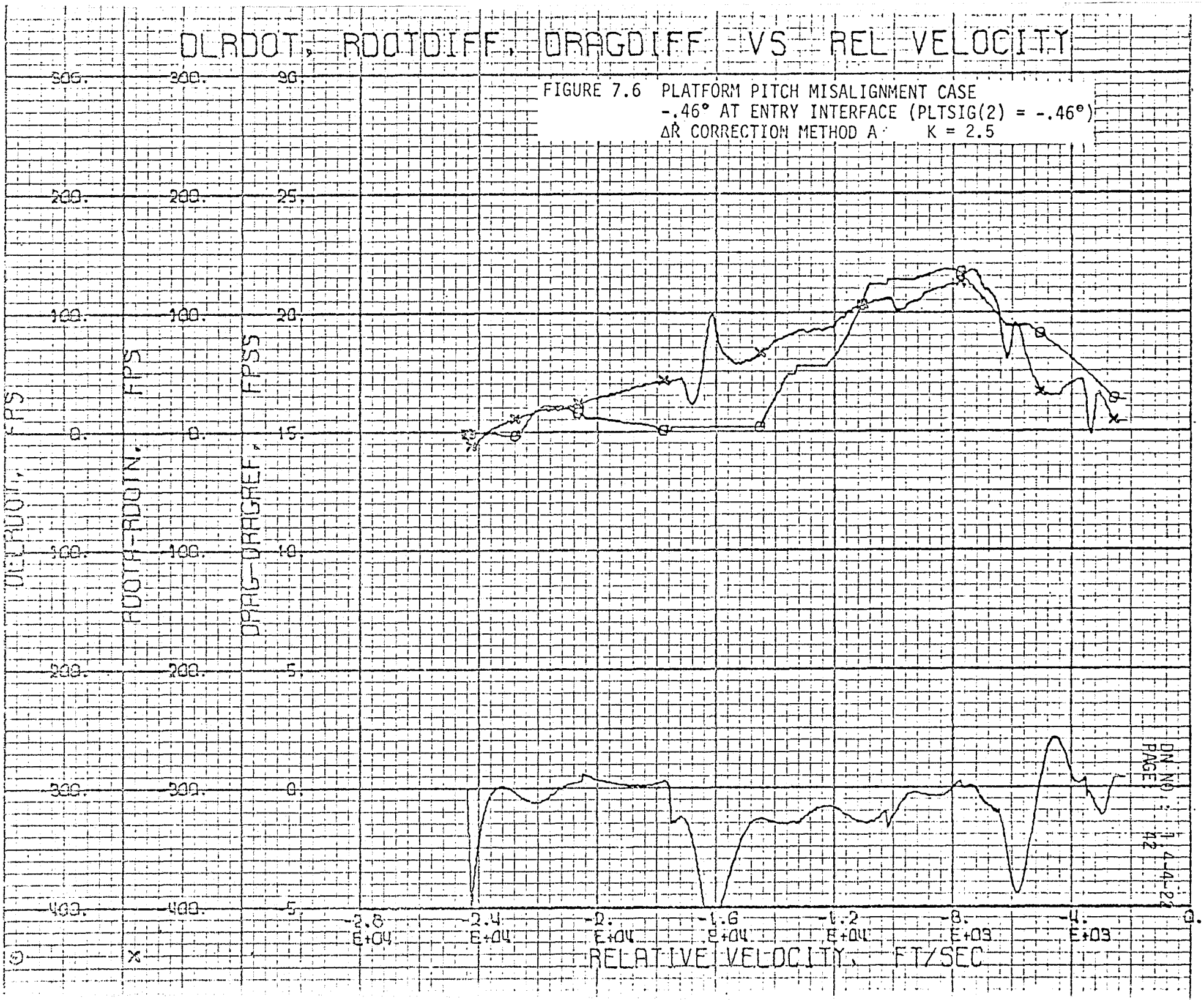
DLRDOT, RDOTDIFF, DRAGDIFF VS REL VELOCITY
FIGURE 7.6 PLATFORM PITCH MISALIGNMENT CASE
-.46° AT ENTRY INTERFACE (PLTSIG(2) = -.46°)
ΔR CORRECTION METHOD A K = 2.5
DLRDOT, FPS
RDOTA-RDOTN, FPS
DRAG-DRAGREF, FPSS
RELATIVE VELOCITY, FT/SEC
-2.8 E+04
-2.4 E+04
-2. E+04
-1.6 E+04
-1.2 E+04
-8. E+03
-4. E+03
0.
DN NO: 1-4-4-22
PAGE: 42

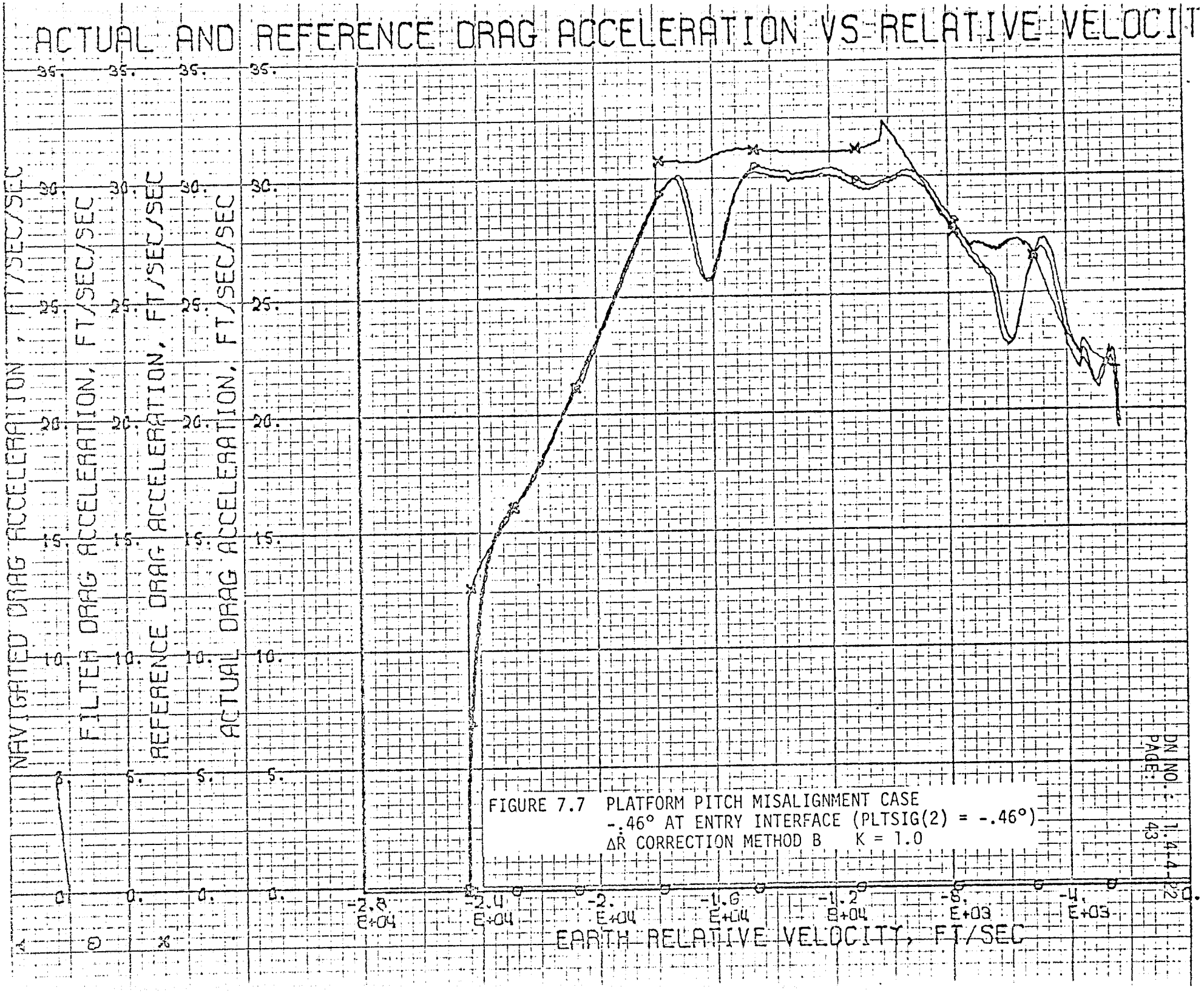

FIGURE 7.7 PLATFORM PITCH MISALIGNMENT CASE
-.46° AT ENTRY INTERFACE (PLTSIG(2) = -.46°)
ΔR CORRECTION METHOD B K = 1.0

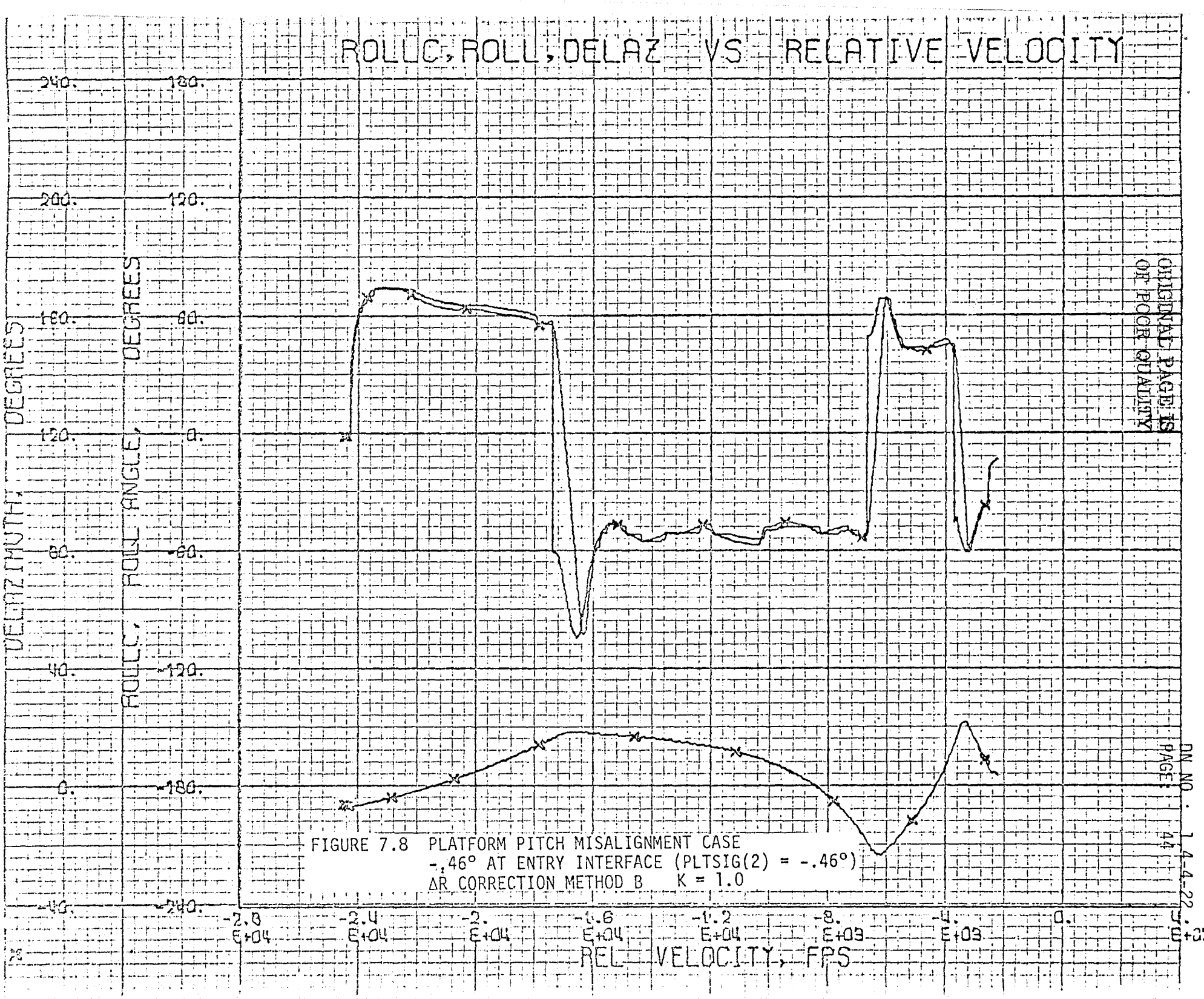

FIGURE 7.8 PLATFORM PITCH MISALIGNMENT CASE
-.46° AT ENTRY INTERFACE (PLTSIG(2) = -.46°)
ΔR CORRECTION METHOD B K = 1.0

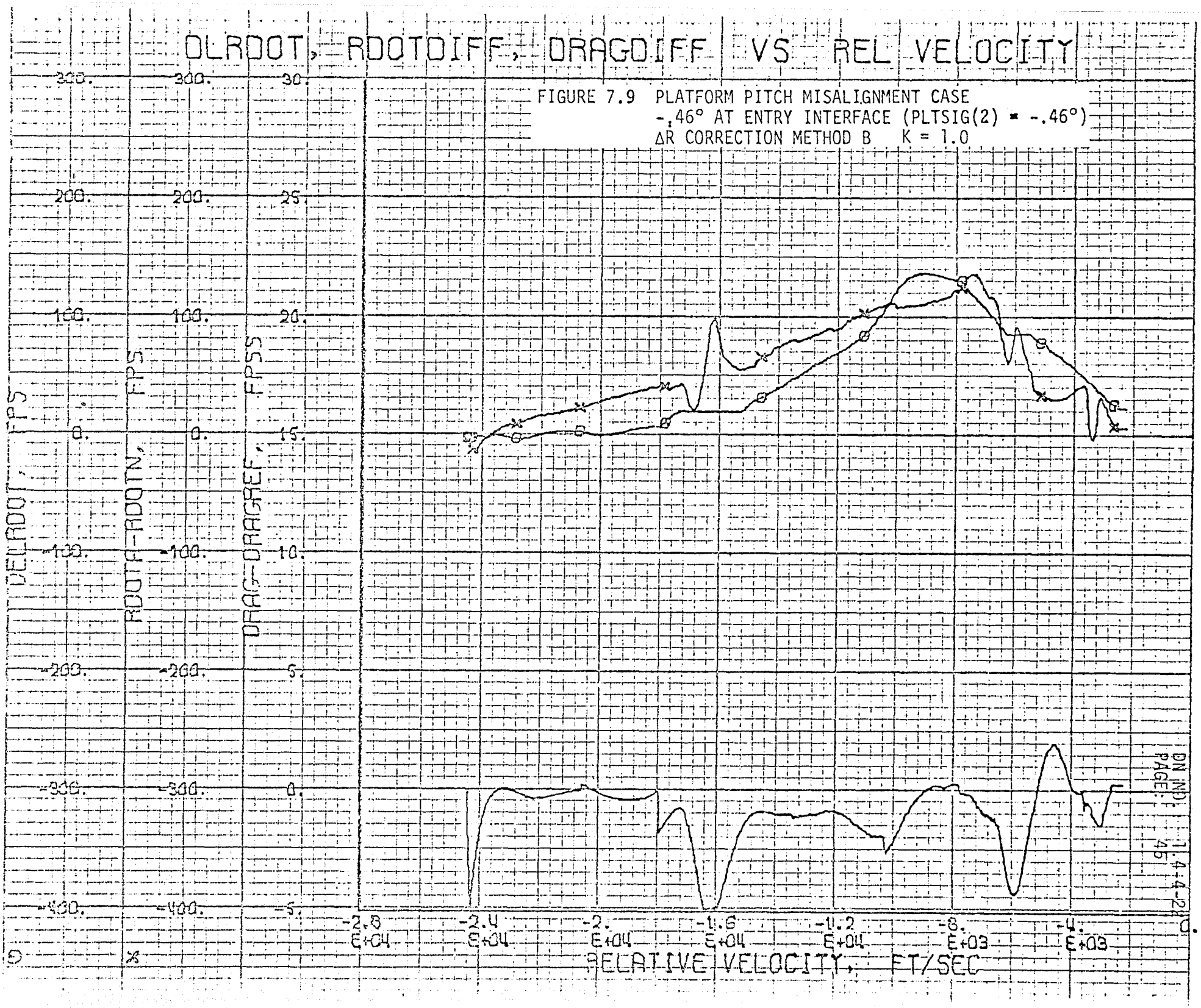
DLRDOT, RDOTDIFF, DRAGDIFF VS REL VELOCITY
FIGURE 7.9 PLATFORM PITCH MISALIGNMENT CASE
-.46° AT ENTRY INTERFACE (PLTSIG(2) = -.46°)
ΔR CORRECTION METHOD B K = 1.0
DELRDOT, FPS
RDOTA-RDOTN, FPS
DRAG-DRAGREF, FPSS
200.
300.
30.
200.
200.
25.
100.
100.
20.
0.
0.
15.
-100.
-100.
10.
-200.
-200.
5.
-300.
-300.
0.
-400.
-400.
-5.
-2.8 E+04
-2.4 E+04
-2. E+04
-1.6 E+04
-1.2 E+04
-8. E+03
-4. E+03
RELATIVE VELOCITY, FT/SEC
DN NO.
PAGE.
14-4-2
45

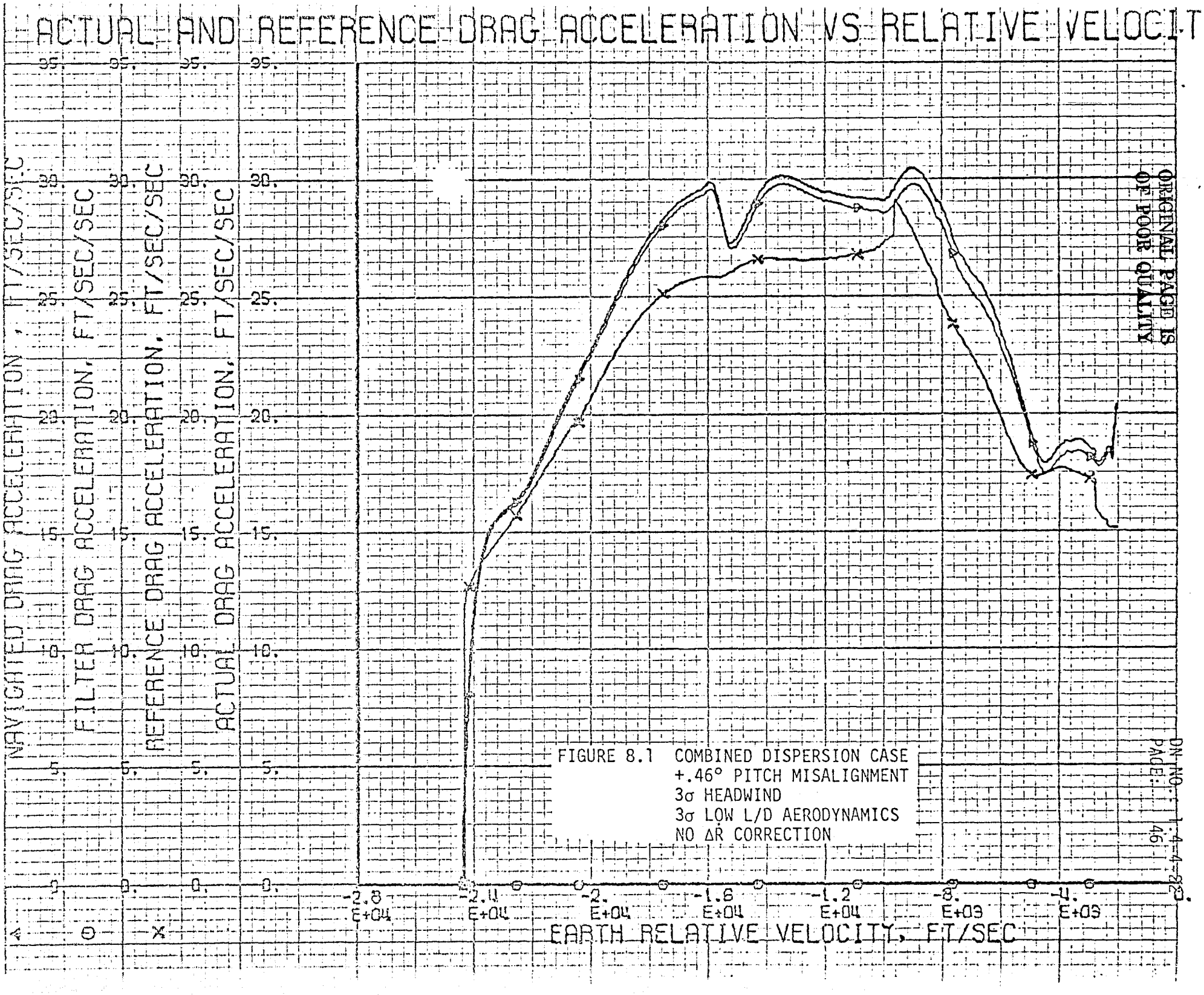

FIGURE 8.1 COMBINED DISPERSION CASE
+.46° PITCH MISALIGNMENT
3σ HEADWIND
3σ LOW L/D AERODYNAMICS
NO ΔR CORRECTION

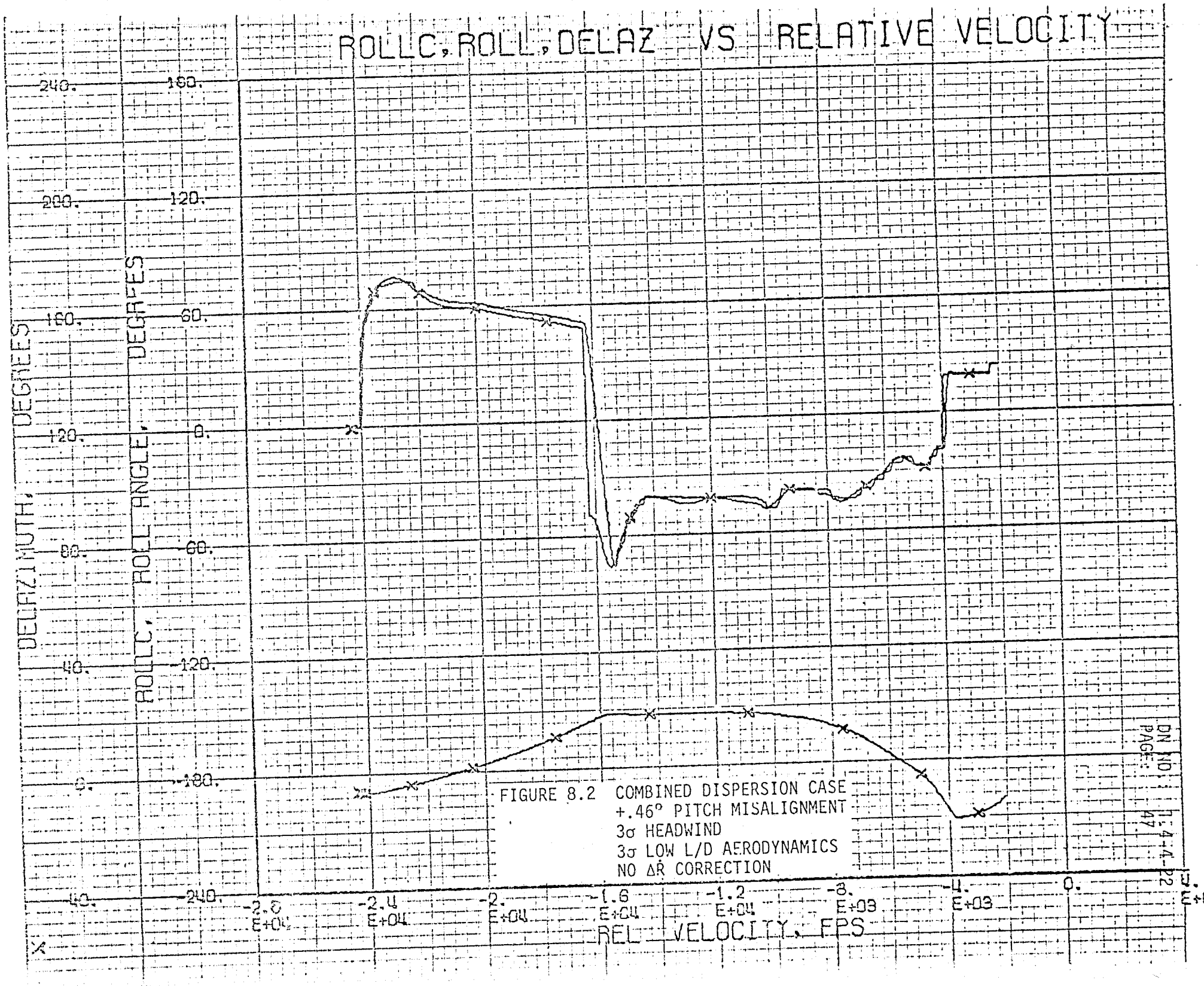

FIGURE 8.2 COMBINED DISPERSION CASE
+.46° PITCH MISALIGNMENT
3σ HEADWIND
3σ LOW L/D AERODYNAMICS
NO $\Delta\dot{R}$ CORRECTION

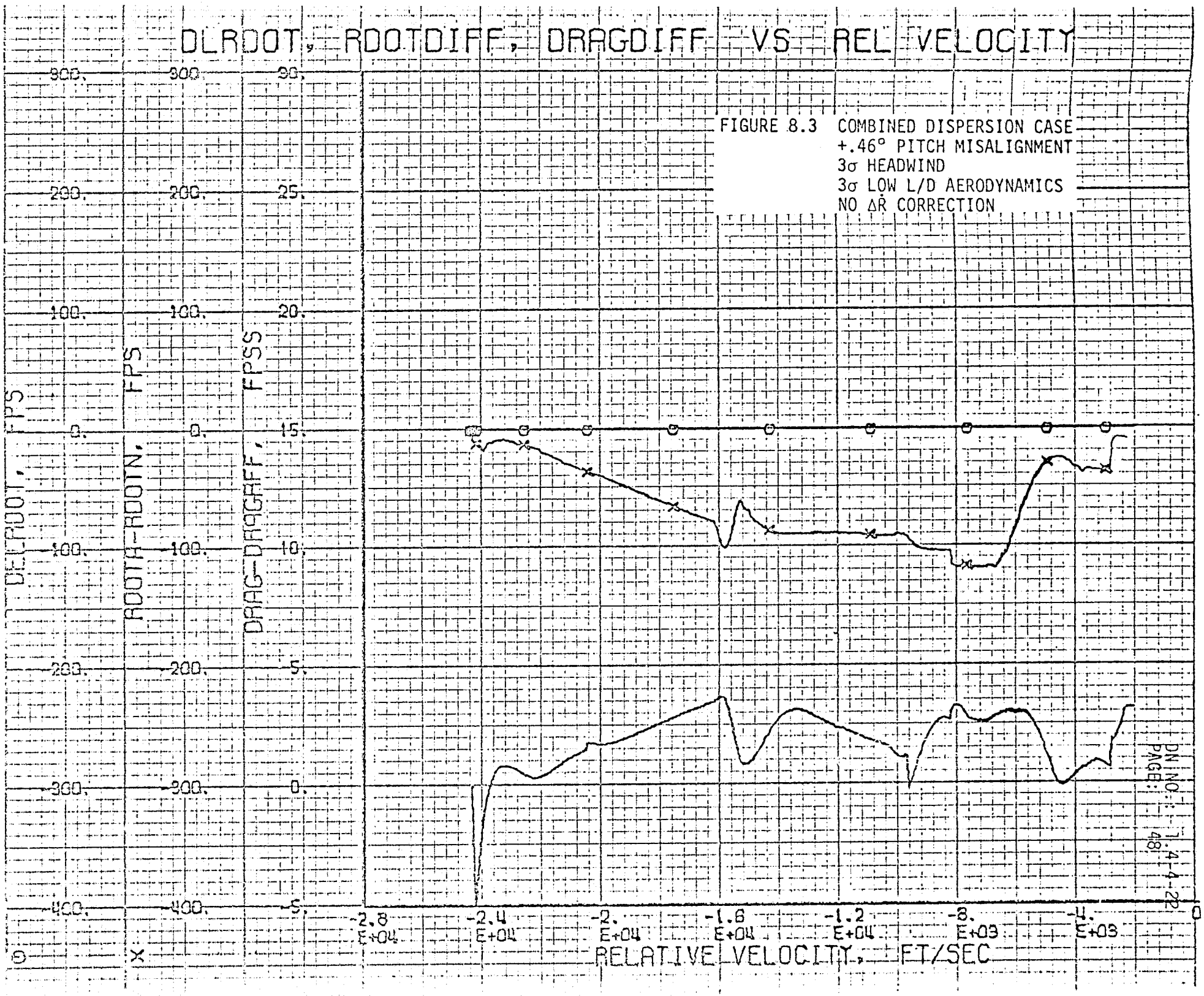

FIGURE 8.3 COMBINED DISPERSION CASE
+.46° PITCH MISALIGNMENT
3σ HEADWIND
3σ LOW L/D AERODYNAMICS
NO $\Delta\dot{R}$ CORRECTION

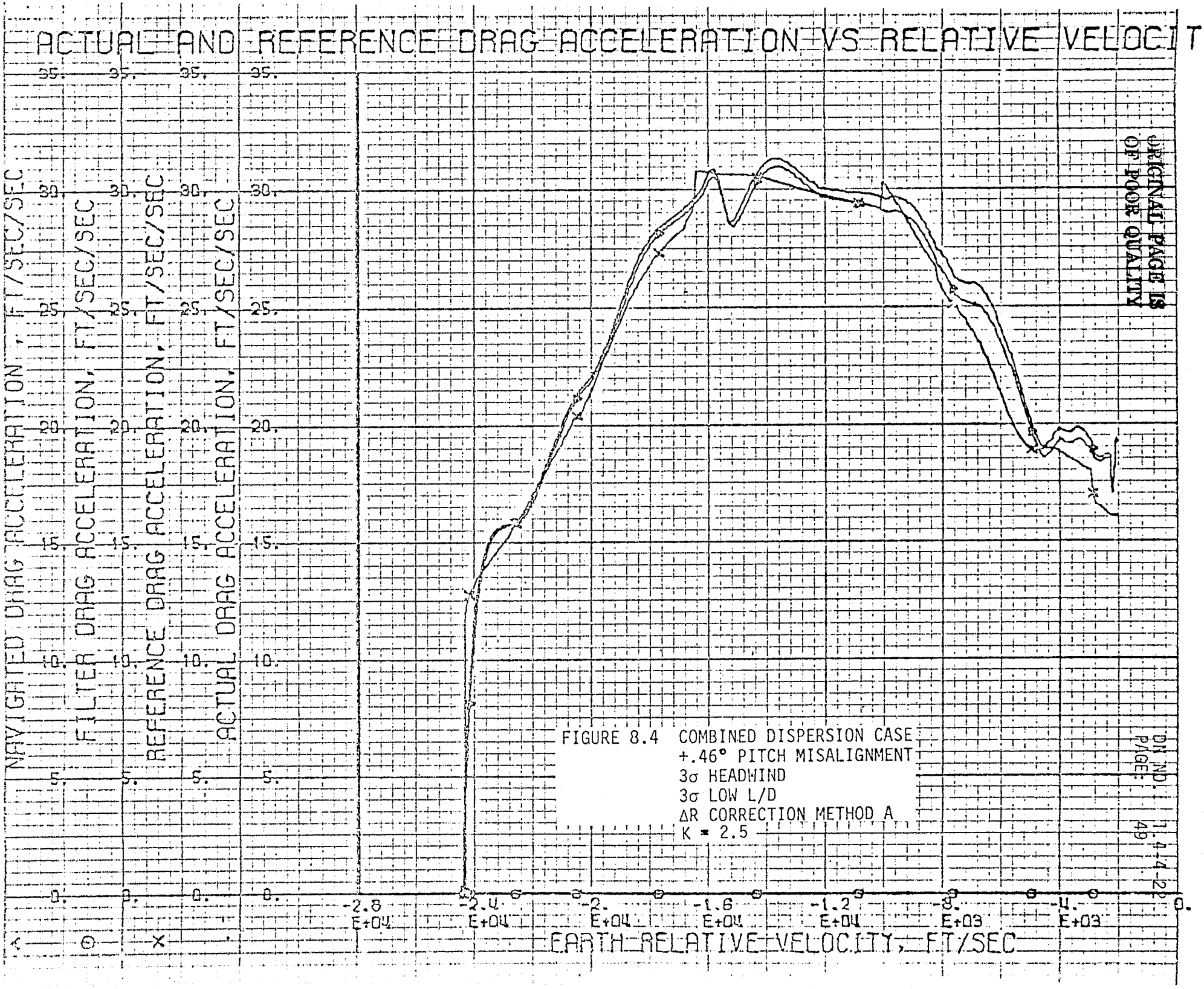

FIGURE 8.4 COMBINED DISPERSION CASE
+.46° PITCH MISALIGNMENT
3σ HEADWIND
3σ LOW L/D
ΔR CORRECTION METHOD A
K = 2.5

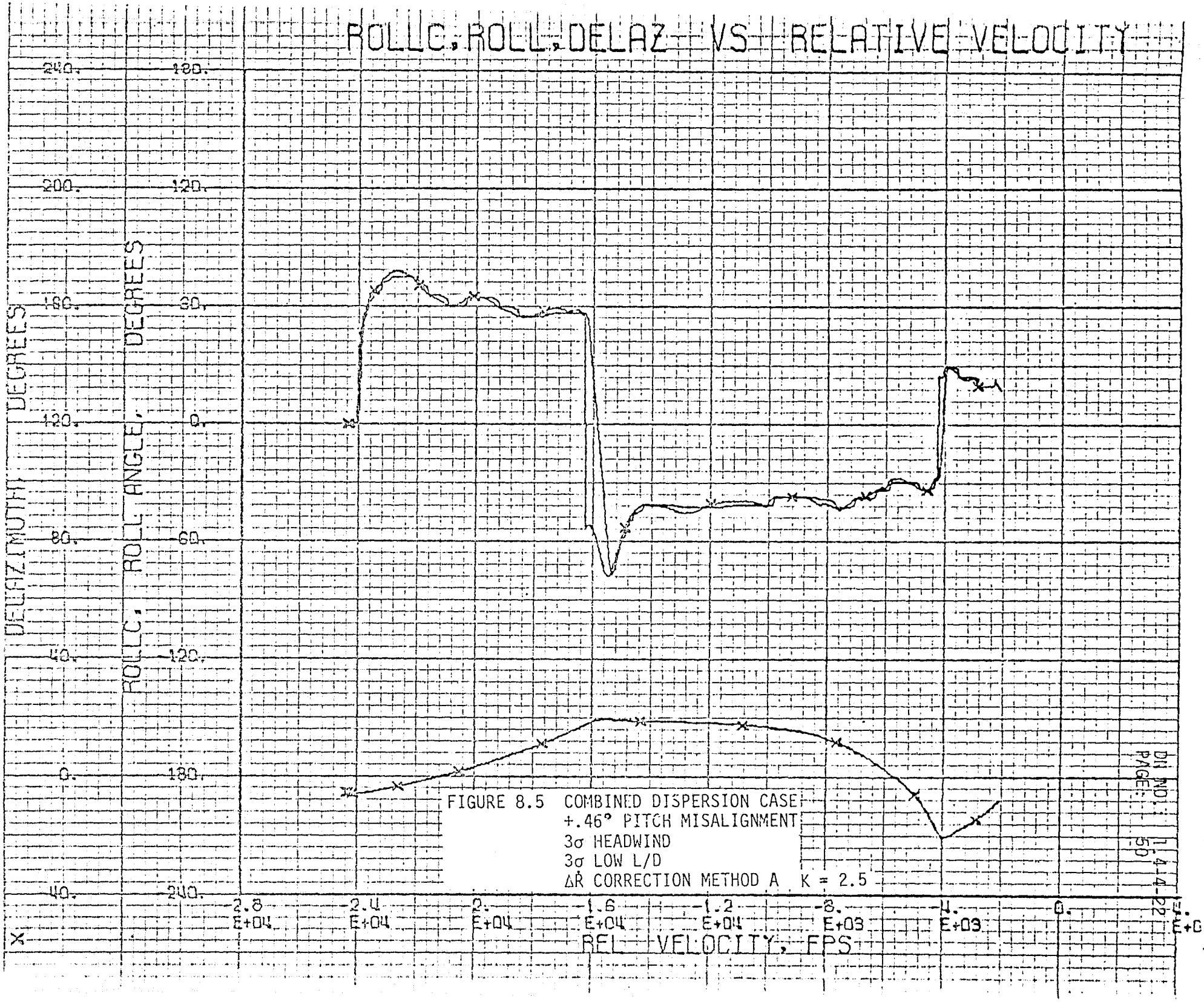

FIGURE 8.5 COMBINED DISPERSION CASE
+.46° PITCH MISALIGNMENT
3σ HEADWIND
3σ LOW L/D
$\Delta\dot{R}$ CORRECTION METHOD A K = 2.5

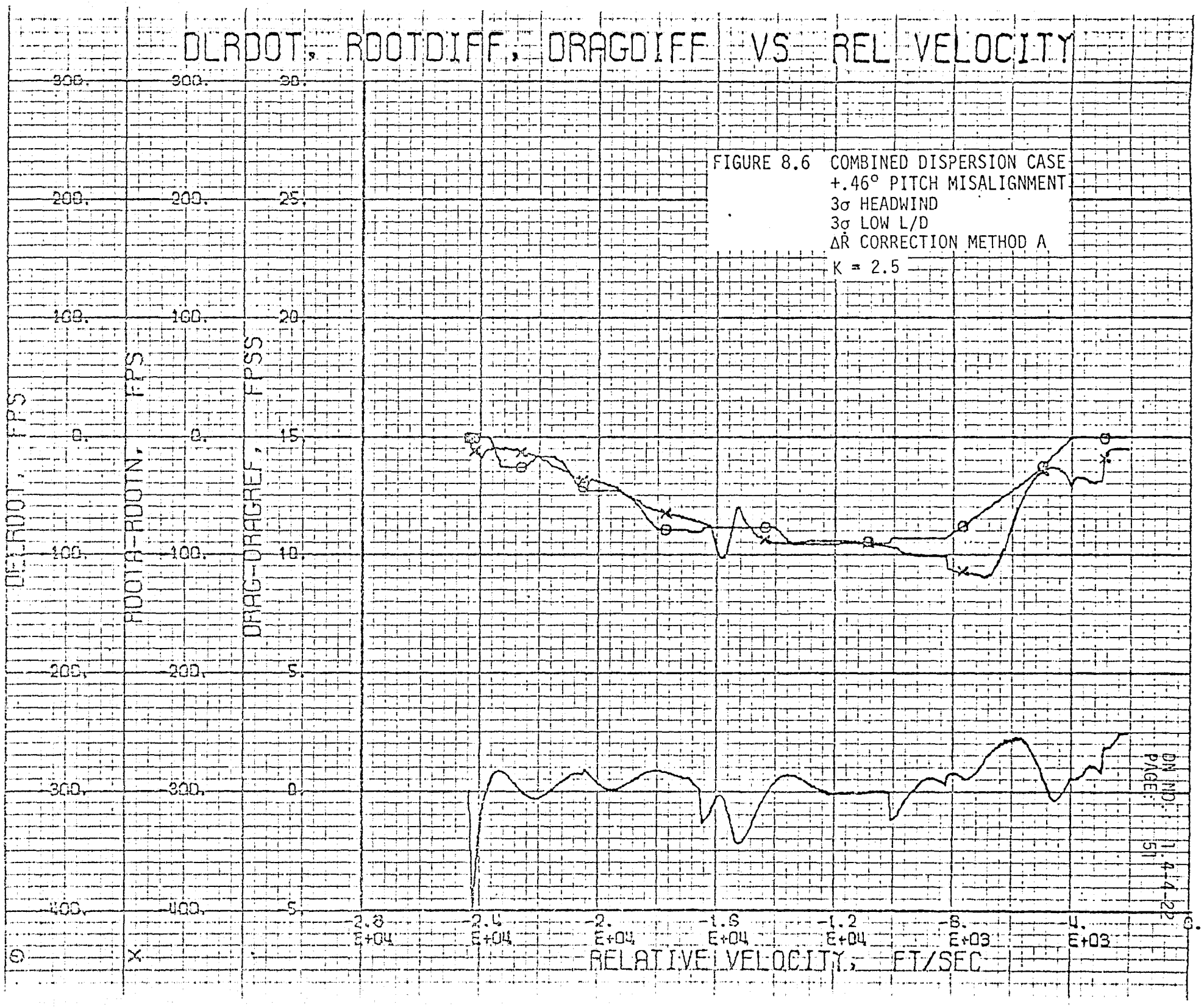
DLRDOT, RDOTDIFF, DRAGDIFF VS REL VELOCITY
FIGURE 8.6 COMBINED DISPERSION CASE
+.46° PITCH MISALIGNMENT
3σ HEADWIND
3σ LOW L/D
ΔṘ CORRECTION METHOD A
K = 2.5
DLRDOT, FPS
RDOTA-RDOTN, FPS
DRAG-DRAGREF, FPSS
RELATIVE VELOCITY, FT/SEC
ON NO. 1 4-4-22
PAGE 51

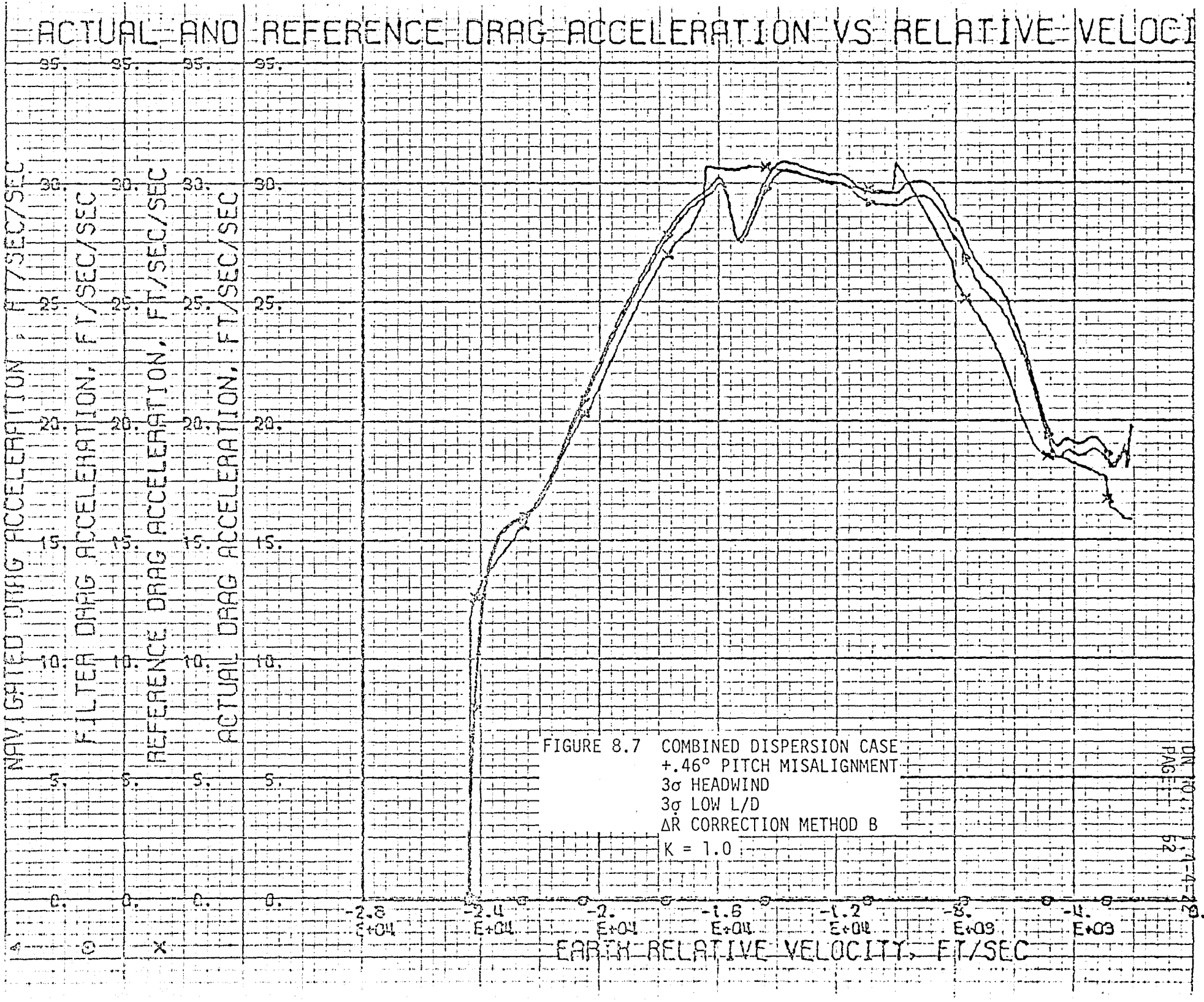

FIGURE 8.7 COMBINED DISPERSION CASE
+.46° PITCH MISALIGNMENT
3σ HEADWIND
3σ LOW L/D
ΔR CORRECTION METHOD B
K = 1.0

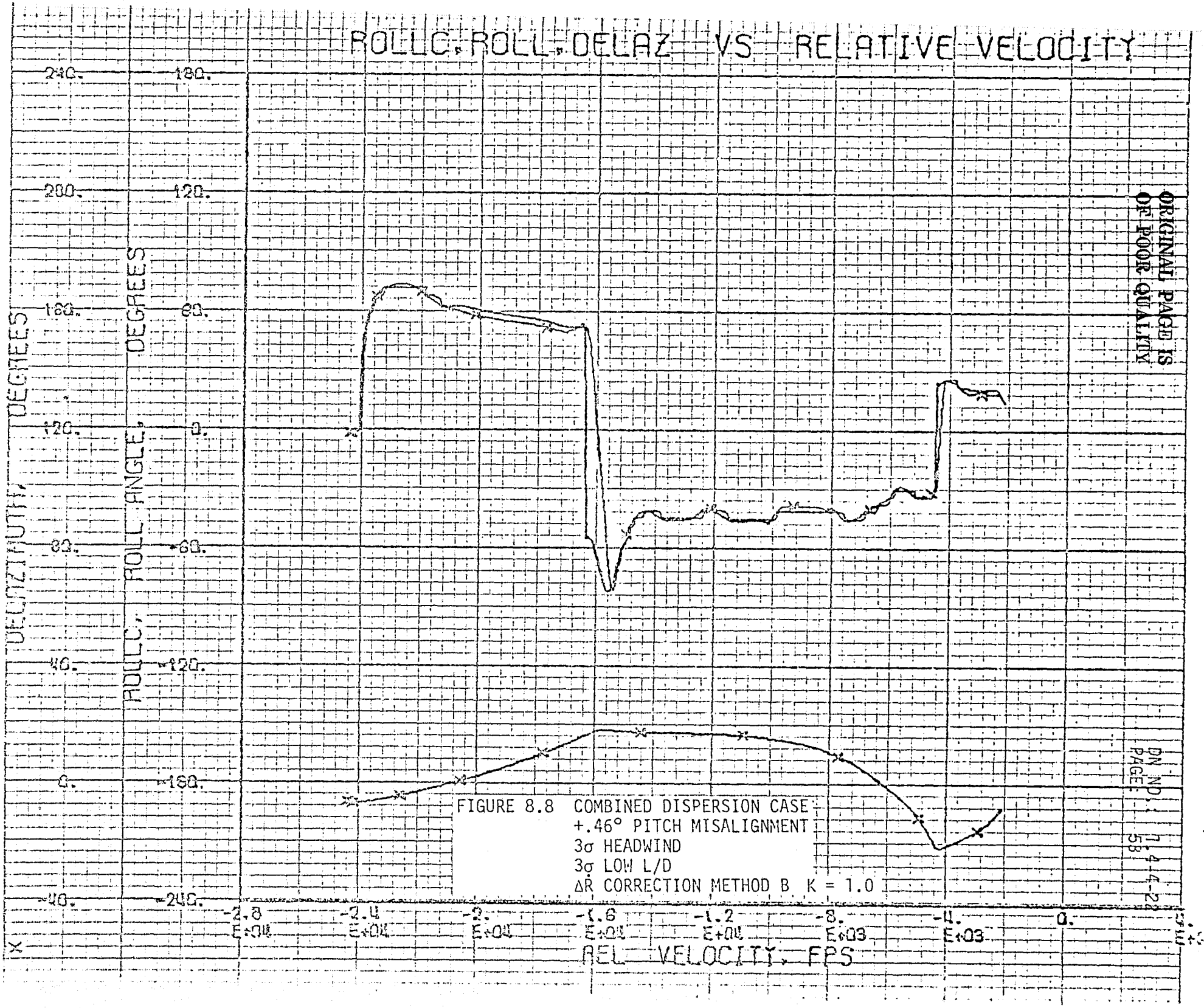

FIGURE 8.8 COMBINED DISPERSION CASE
+.46° PITCH MISALIGNMENT
3σ HEADWIND
3σ LOW L/D
ΔR CORRECTION METHOD B K = 1.0

CONTINUED ON NEXT PAGE

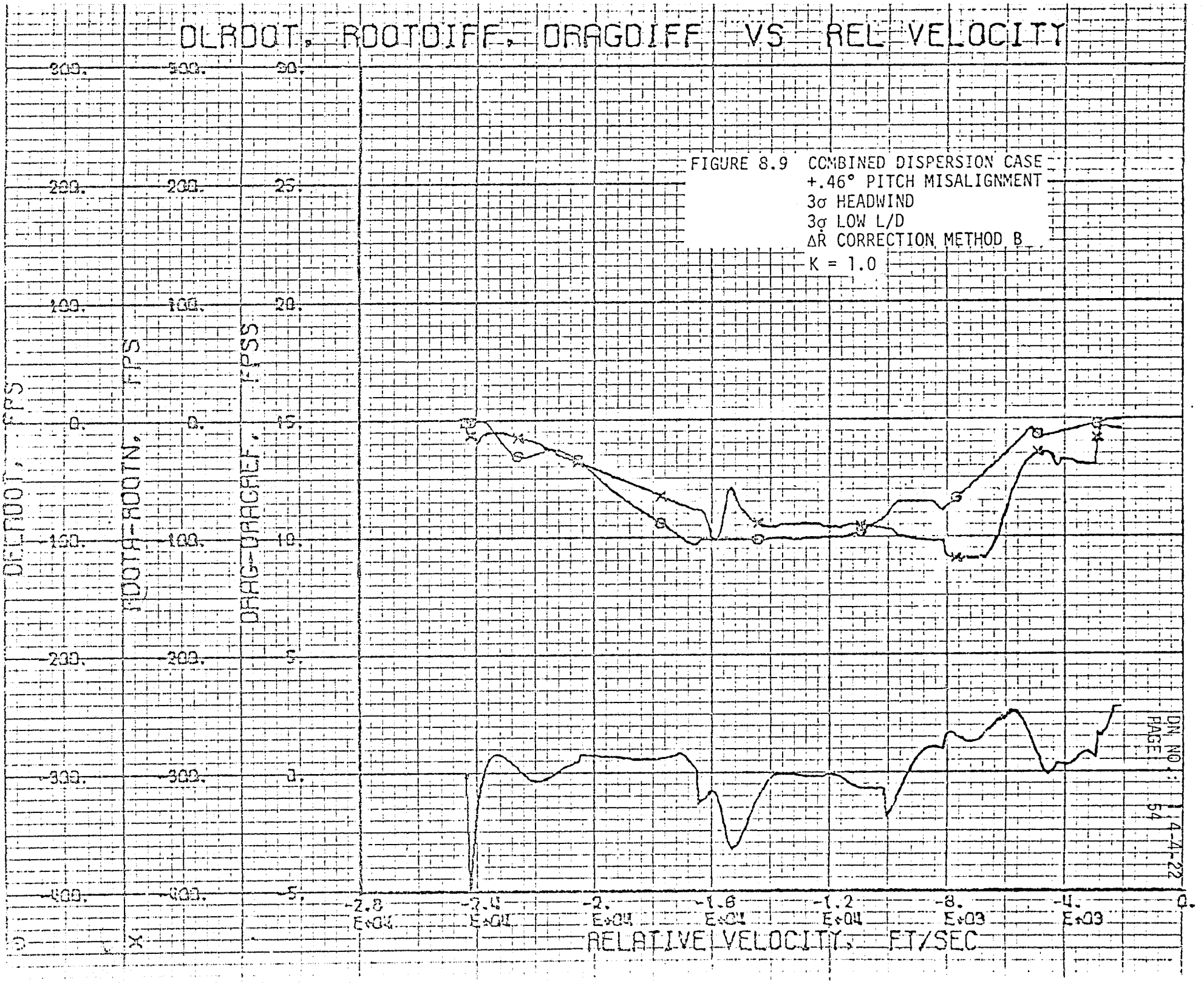
DLRDOT, ROOTDIFF, DRAGDIFF VS REL VELOCITY
FIGURE 8.9 COMBINED DISPERSION CASE
+.46° PITCH MISALIGNMENT
3σ HEADWIND
3σ LOW L/D
ΔR CORRECTION METHOD B
K = 1.0
DLRDOT, FPS
ROOTR-ROOTN, FPS
DRAG-DRAGREF, FPSS
RELATIVE VELOCITY, FT/SEC
DN NO: 14-4-22
PAGE 54

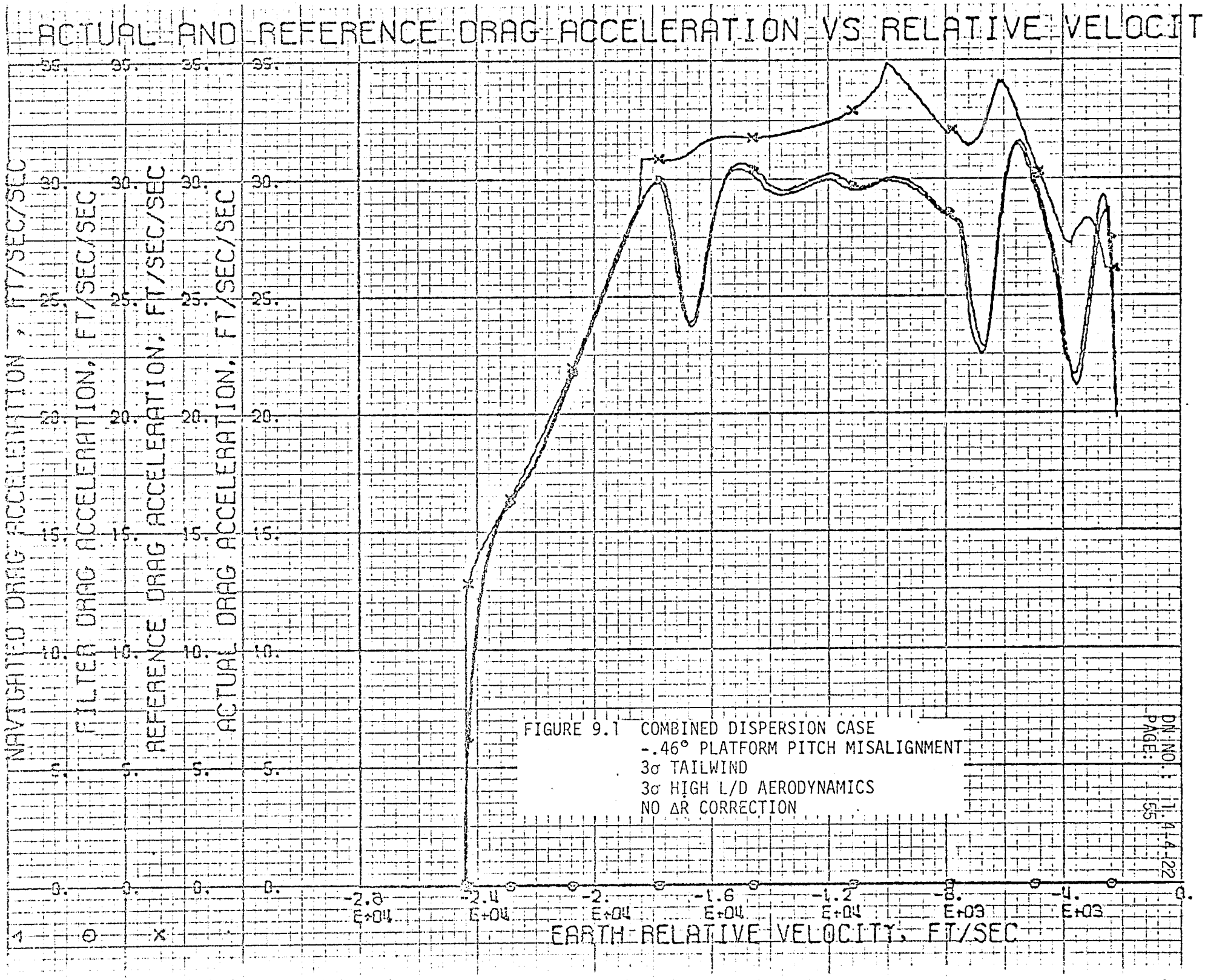

FIGURE 9.1 COMBINED DISPERSION CASE
-.46° PLATFORM PITCH MISALIGNMENT
3σ TAILWIND
3σ HIGH L/D AERODYNAMICS
NO ΔR CORRECTION

DN NO.: 11-4-22
PAGE: 55

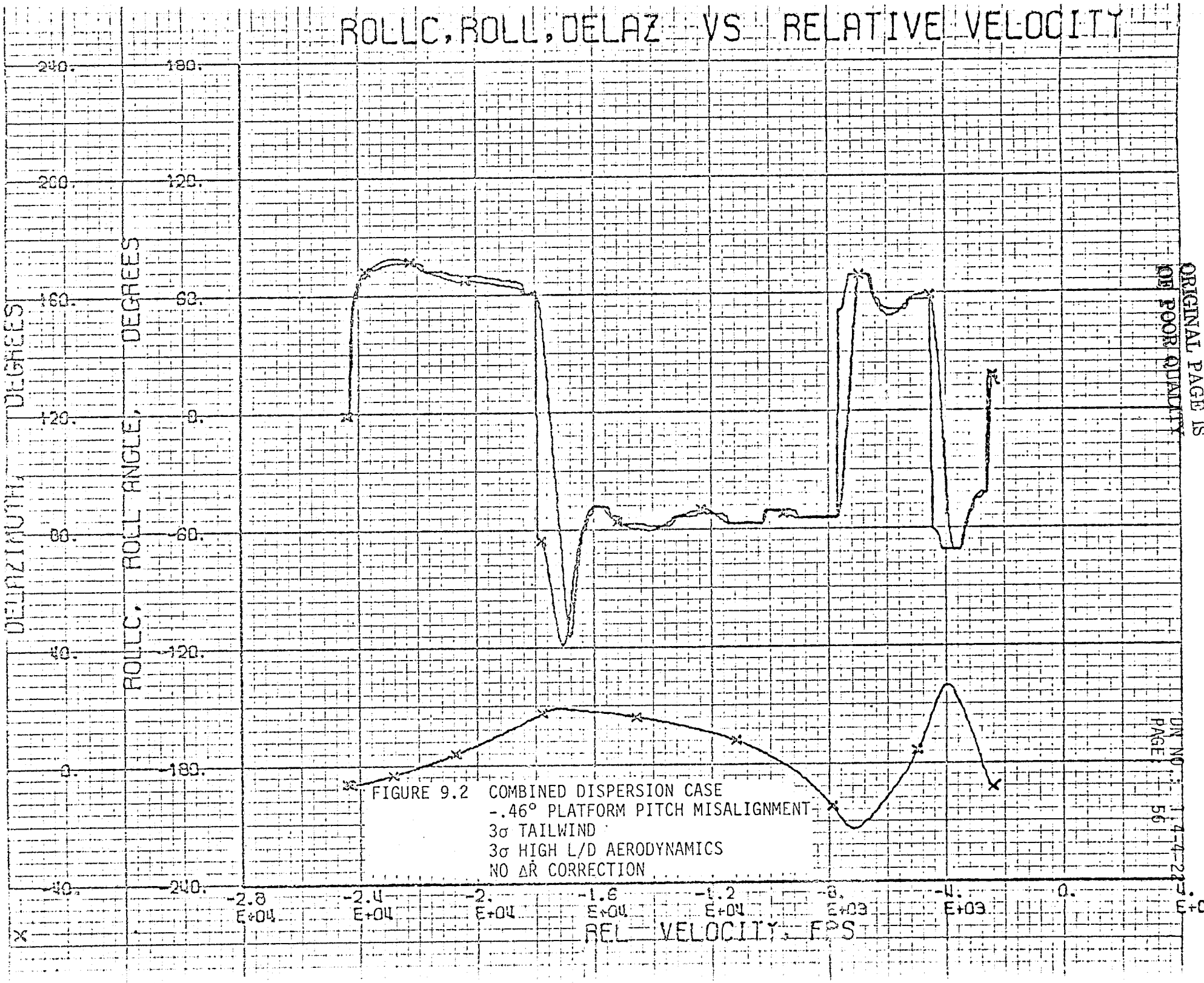

FIGURE 9.2 COMBINED DISPERSION CASE
-.46° PLATFORM PITCH MISALIGNMENT
3σ TAILWIND
3σ HIGH L/D AERODYNAMICS
NO ΔR CORRECTION

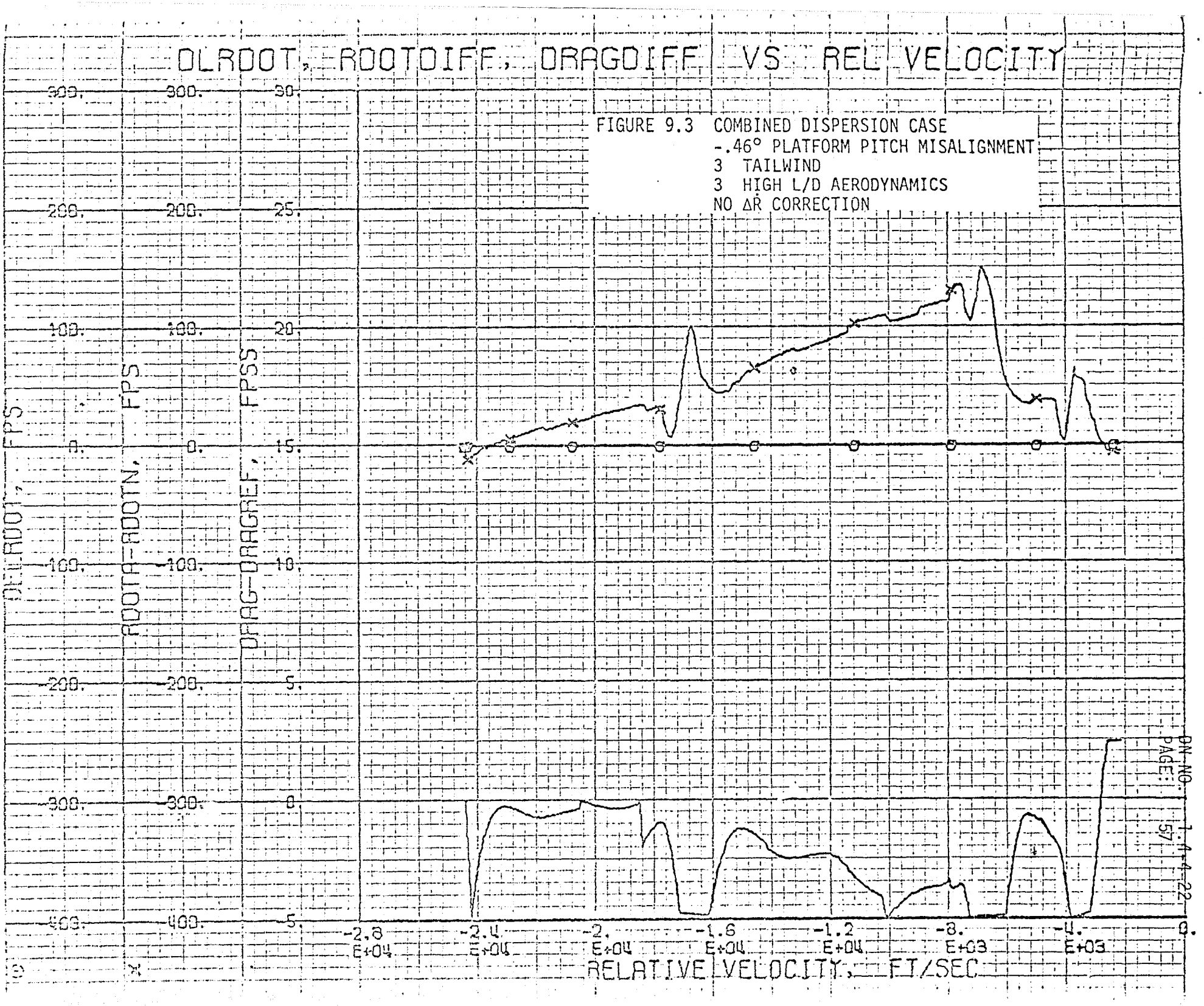
DLROOT, ROOTDIFF, DRAGDIFF VS REL VELOCITY
FIGURE 9.3 COMBINED DISPERSION CASE
-.46° PLATFORM PITCH MISALIGNMENT
3 TAILWIND
3 HIGH L/D AERODYNAMICS
NO ΔR CORRECTION
DLROOT, FPS
ROOTA-ROOTN, FPS
DRAG-DRAGREF, FPSS
300.
200.
100.
0.
-100.
-200.
-300.
-400.
30.
25.
20.
15.
10.
5.
0.
-5.
-2.8 E+04
-2.4 E+04
-2. E+04
-1.6 E+04
-1.2 E+04
-8. E+03
-4. E+03
0.
RELATIVE VELOCITY, FT/SEC
DN NO. 1-4-22
PAGE 57

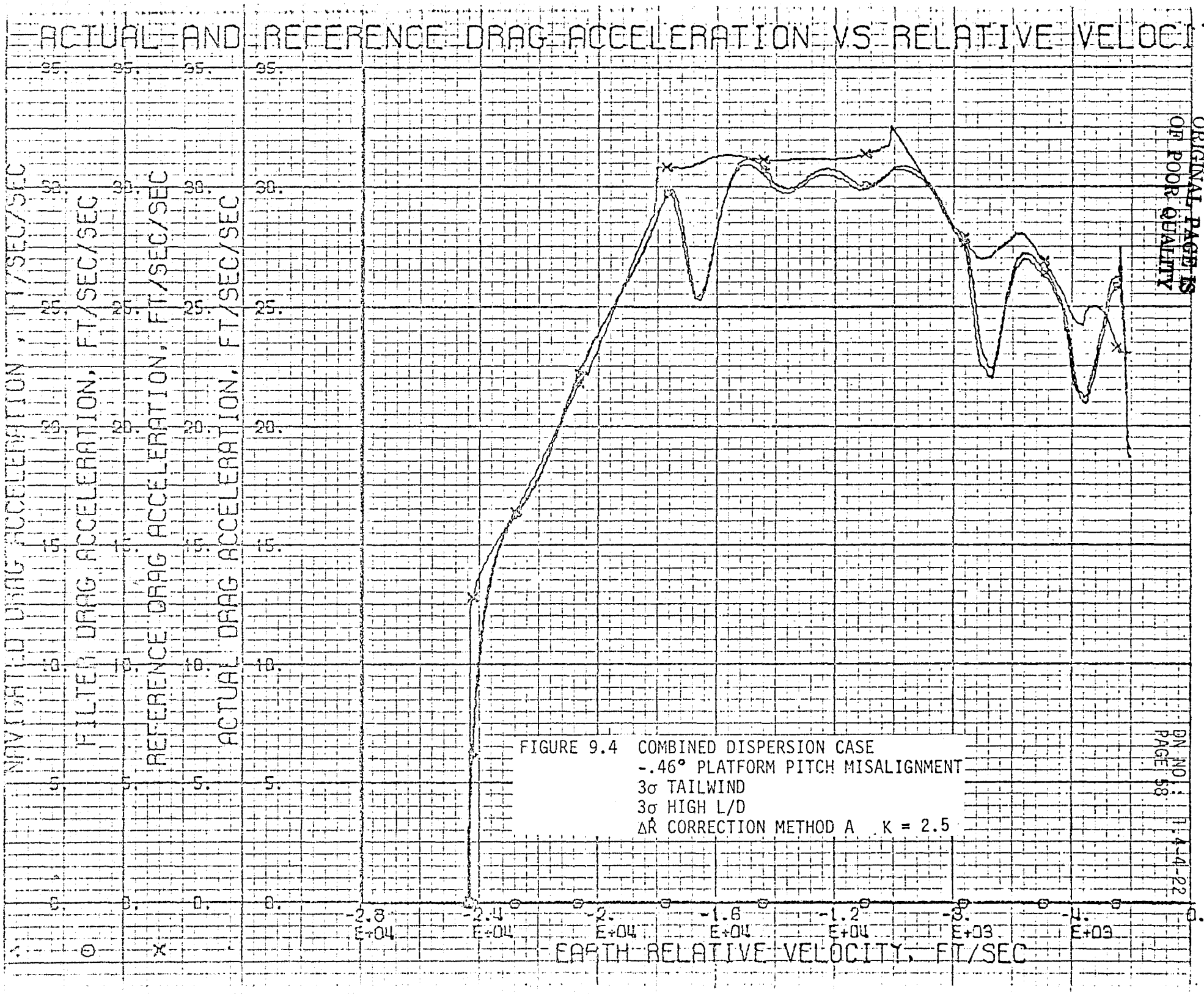

FIGURE 9.4 COMBINED DISPERSION CASE
-.46° PLATFORM PITCH MISALIGNMENT
3σ TAILWIND
3σ HIGH L/D
$\Delta\dot{R}$ CORRECTION METHD A K = 2.5

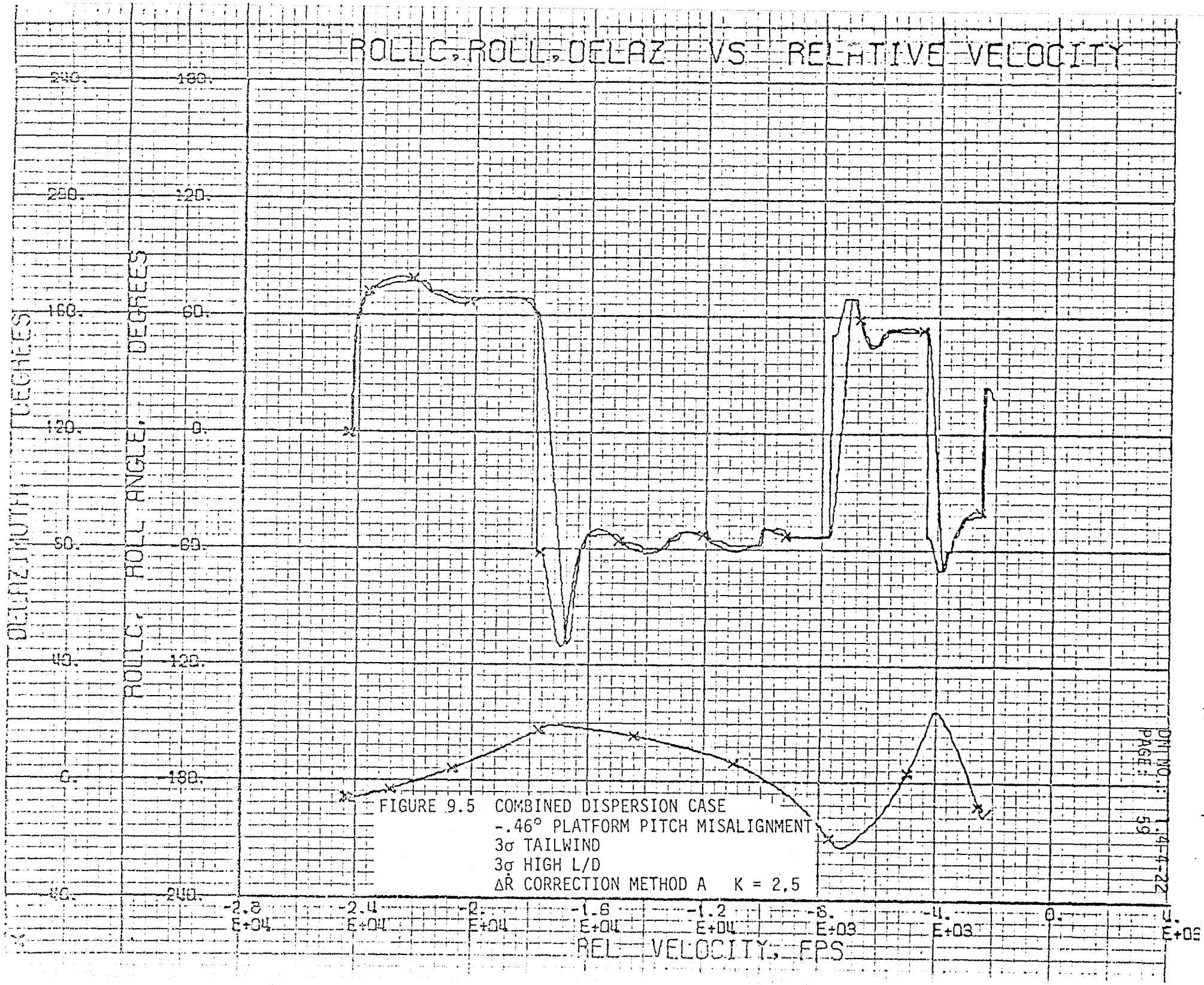

FIGURE 9.5 COMBINED DISPERSION CASE
-.46° PLATFORM PITCH MISALIGNMENT
3σ TAILWIND
3σ HIGH L/D
ΔR CORRECTION METHOD A K = 2,5

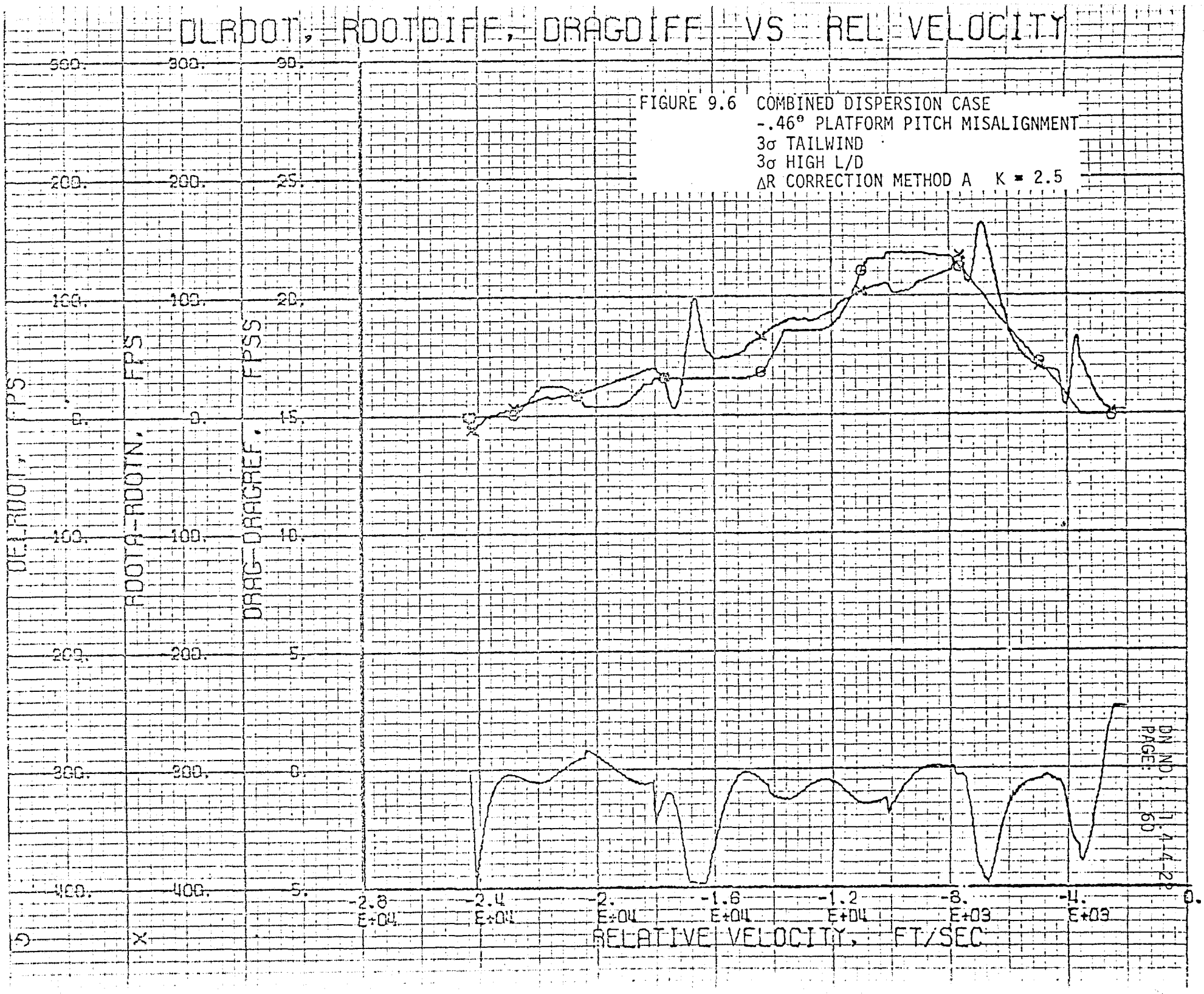
DLRDOT, RDOTDIFF, DRAGDIFF VS REL VELOCITY
FIGURE 9.6 COMBINED DISPERSION CASE
-.46° PLATFORM PITCH MISALIGNMENT
3σ TAILWIND
3σ HIGH L/D
ΔR CORRECTION METHOD A K = 2.5
DELRDOT, FPS
RDOTQ-RDOTN, FPS
DRAG-DRAGREF, FPSS
RELATIVE VELOCITY, FT/SEC
-2.8 E+04
-2.4 E+04
-2. E+04
-1.6 E+04
-1.2 E+04
-8. E+03
-4. E+03
0.
DN NO. 1-4-4-2
PAGE 160

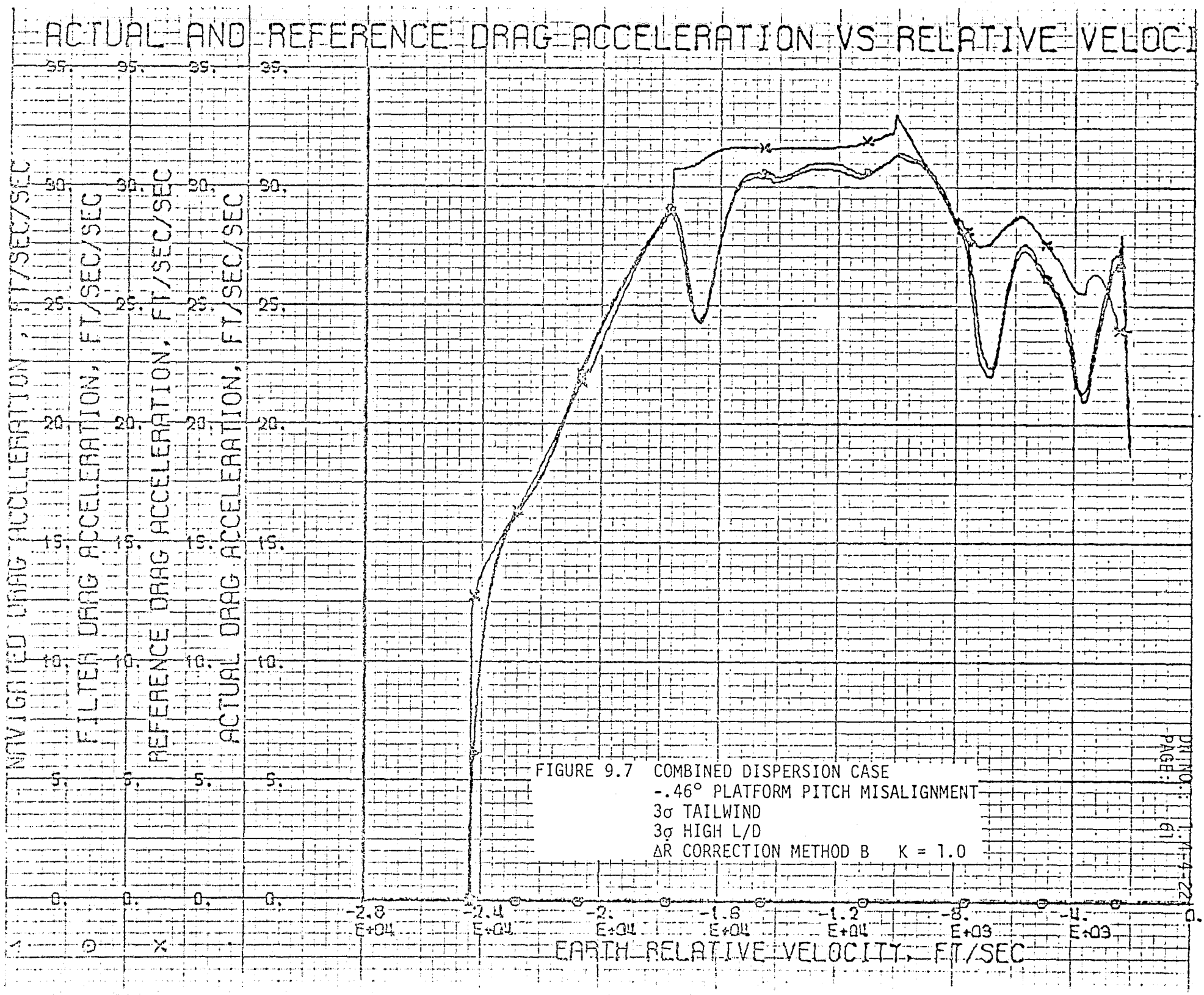

FIGURE 9.7 COMBINED DISPERSION CASE
-.46° PLATFORM PITCH MISALIGNMENT
3σ TAILWIND
3σ HIGH L/D
$\Delta\dot{R}$ CORRECTION METHOD B K = 1.0

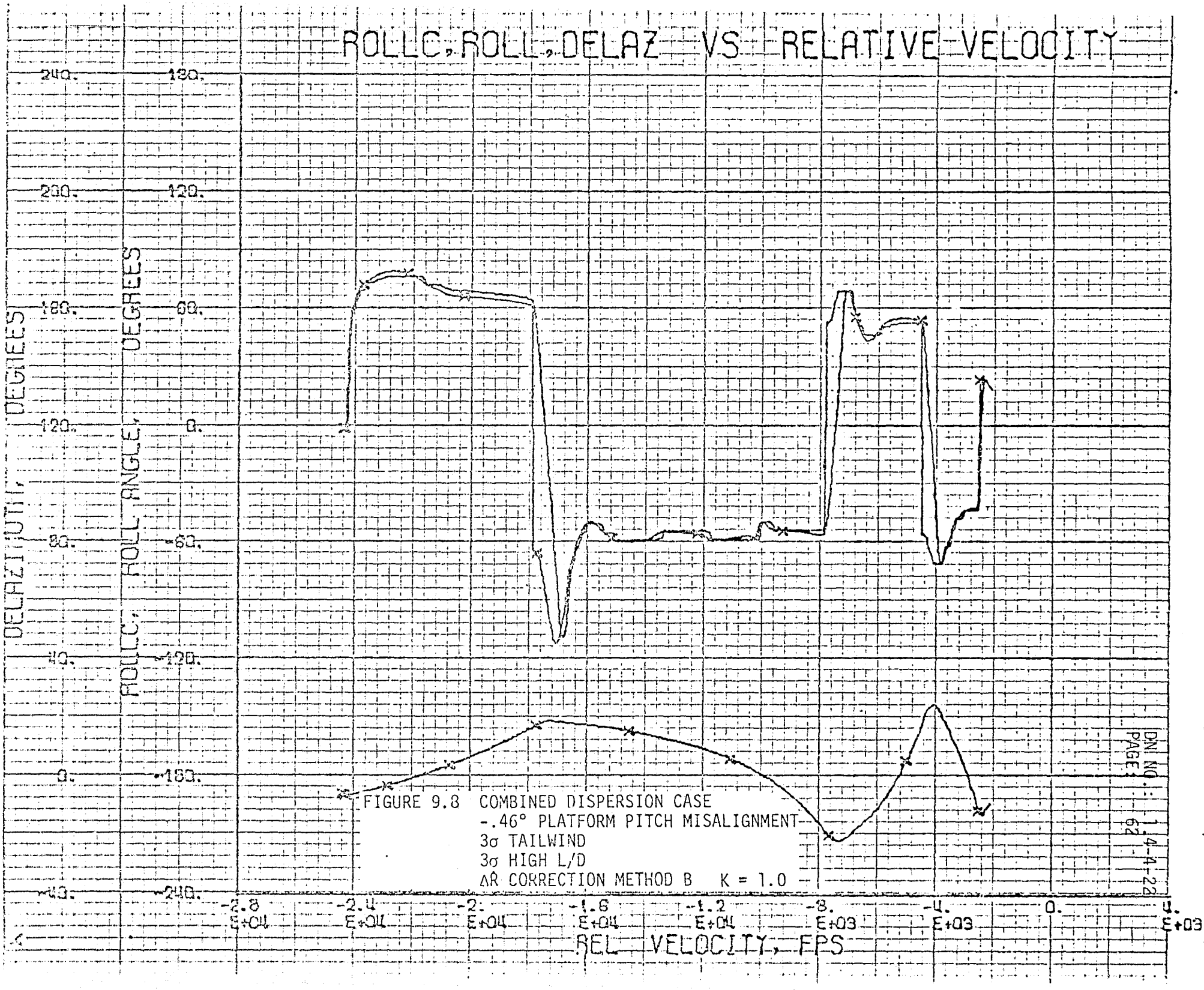

FIGURE 9.8 COMBINED DISPERSION CASE
-.46° PLATFORM PITCH MISALIGNMENT
3σ TAILWIND
3σ HIGH L/D
$\Delta\hat{R}$ CORRECTION METHOD B K = 1.0

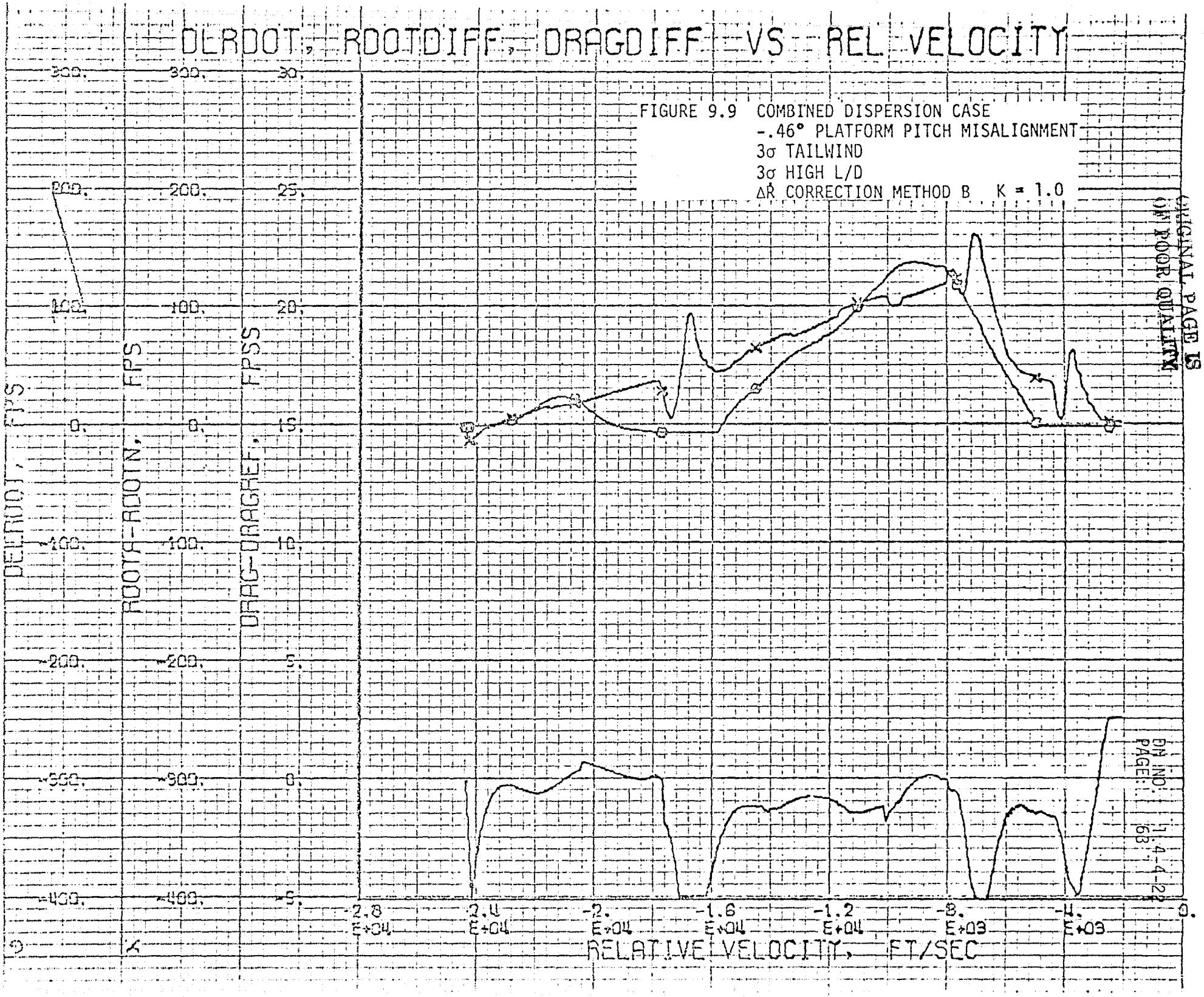

FIGURE 9.9 COMBINED DISPERSION CASE
-.46° PLATFORM PITCH MISALIGNMENT
3σ TAILWIND
3σ HIGH L/D
ΔR CORRECTION METHOD B K = 1.0

ORIGINAL PAGE IS
OF POOR QUALITY

DN IND.
PAGE: 7-4-4-22
63

5.0 CONCLUSIONS

The $\Delta\dot{R}$ correction to the guidance controller equation utilizing the drag integral feedback concept enables the vehicle guidance system to more accurately command roll angles to follow the reference drag profile. This has been demonstrated by SVDS simulations incorporating various error sources including dispersions in atmosphere, aerodynamics, navigation information, and vehicle roll angle. Both integral feedback methods studied produce favorable results.

6.0 RECOMMENDATIONS

It is recommended that the drag feedback method A be implemented into the ADC guidance flight software. If later study shows the convergence/divergence test in method A is not needed, this check may be deleted at that time. Further study should be conducted (1) to further optimize the gain/gains used and (2) to account for the large navigation updates during the last part of the entry.

7.0 REFERENCES

A. Harpold, Jon C.: "Analytic Drag Control Entry Guidance System," Revision 1, Johnson Space Center Internal Note No. 74-FM-25, 21 January 1976.

B. Software Development Branch, "Space Vehicle Dynamics Simulation (SVDS) Program Description," Johnson Space Center Internal Note No. 76-FM-26, 6 May 1976.

C. Rich, T. M.: "JSC IMU Error Model Revisions; New Thresholds for Tracking Test and SPRT 2-IMU FDI," MDTSCO Working Paper No. E914-8A-028, 10 May 1976.